

GPO PRICE \$ _____

CFSTI PRICE(S) \$ _____

Hard copy (HC) \$3.00

Microfiche (MF) .75

ff 653 July 65

PROGRESS AND PROBLEMS IN ATMOSPHERE ENTRY

By Alfred J. Eggers, Jr., and Nathaniel B. Cohen

Office of Advanced Research and Technology
National Aeronautics and Space Administration
Washington, D.C.

FACILITY FORM 802

N66 29405

(ACCESSION NUMBER)

(THRU)

72

(PAGES)

1

(CODE)

TMX-56855

(NASA CR OR TMX OR AD NUMBER)

30

(CATEGORY)

Presented at the XVith IAF International Congress,
Athens, Greece, September 13-18, 1965.

PROGRESS AND PROBLEMS IN ATMOSPHERE ENTRY

By Alfred J. Eggers, Jr., and Nathaniel B. Cohen

ABSTRACT


29405

Problems of entry vehicle motion, heating, and heat protection are discussed in the context of current and possible future space flight missions, including unmanned probes of the atmospheres of Mars, Venus, and Jupiter, and manned vehicles appropriate for controlled planetary entry at velocities from orbital to hyperbolic. Recent advances in reentry physics, including both theoretical and experimental work in flow field analysis, convective and radiative heating, and combined effects, have enhanced our ability to predict aerodynamic heating. Problems in reentry physics which remain, such as transition to turbulent flow, ~~to~~ heat transfer at hyper-velocities, and complex radiation flow-field interactions and their possible influence on vehicle configuration are discussed. Attention is also given to ground simulation facilities, such as the expansion tunnel, ballistic shock tunnel, and high enthalpy arc jet, which are particularly useful in the solution of problems in reentry physics and heat shield materials behavior. Finally, some consideration is given to the comparative features of rocket braking and maneuvering as contrasted to atmosphere braking and maneuvering for the spectrum of speeds and mission profiles of future interest.

INTRODUCTION

Significant advances have been accomplished in the science and technology appropriate to atmosphere entry of spacecraft during the eight years since the launching of Sputnik I. This progress is no better illustrated than by the successful entry from earth orbit of the manned Vostok, Mercury, Voskhod, and Gemini spacecraft, for which the problems inherent in orbital entry, such as high convective heating rate and load and communication blackout, were successfully overcome. For the past four years, atmosphere entry research activities in the United States were concentrated upon the problems appropriate to return from lunar missions which are characterized, for the Apollo vehicle, by nonnegligible radiative heating rates and a highly nonsymmetric flow field, as well.

Although the first Apollo vehicle entry has yet to be demonstrated, the next few years are expected to bring successful accomplishment of first earth orbital and then lunar return entries with this vehicle. Much engineering work for this vehicle remains to be done; however, the fundamental research activity associated with Apollo is being reduced in favor of that associated with missions and vehicles of the more distant future. Already certain new problems arising in such missions have been investigated in the various laboratories, resulting in important new knowledge. It is the purpose of this paper to discuss some of the more interesting missions of the future,



to describe those mission characteristics pertinent to atmosphere entry, to review some related research accomplishments in the recent literature, and to point out some of the many problems remaining to be solved.

References cited throughout the paper are merely representative of the wealth of literature available on the topics discussed. An extensive bibliography was provided by Love (ref. 1). Additional material may be found in the reference lists of the cited papers.

FUTURE MISSIONS

The post-Apollo era is likely to provide a variety of new entry opportunities which introduce a number of phenomena considerably different from those related to near-ballistic entries at orbital or escape velocities into the Earth's atmosphere. The establishment of long-duration earth-orbital laboratories may well lead to a requirement for logistic vehicles capable of generating a sufficient lift/drag ratio to provide for reduced entry decelerations, maneuvering during entry for longitudinal and lateral ranging, and horizontal landing capability. Such vehicles would, of necessity, be relatively slender and nonsymmetric in order to provide the required lift; the economics of such vehicles might call for required re-use. While the gross entry environment for these

vehicles will be little different from that previously encountered, their configurations will result in flow fields of a somewhat different character.

We are presently fast approaching the capability of launching unmanned probes of the atmospheres of Mars and Venus, for which a whole host of new entry problems will be encountered. The atmospheres of these two planets are at this time not fully determined, but both are thought to contain significant fractions of CO_2 and N_2 , leading us to expect radiation heat transfer of major proportion from cyanogen formed in the shock layer, especially at the moderate velocities associated with Mars entry. Characteristic entry velocities for such probes are shown in Figure 1.

Because Mars is thought to be that planet in the solar system, other than Earth, most likely to have an environment suitable for the evolution of life, it may be the subject of extensive exploration, first by unmanned systems, and then, if warranted, by man. The mounting of a manned exploration program will be accompanied by major new problems in atmosphere entry associated with the three types of entry vehicles contemplated for use in such a mission; namely, a large vehicle capable of hyperbolic entry into the Martian atmosphere as alternative to a propulsive maneuver, an excursion module for landing on the surface from orbit if the Mars Orbital Rendezvous mode is used, and a hyperbolic earth

reentry module. The entry velocity range associated with each of these maneuvers is shown in Figure 1. Earth return velocities shown presuppose use of trajectories shaped by passage close to Venus during the mission. For direct trajectories, earth return velocities up to about 23 km/sec are appropriate.

Also listed in the figure is the entry velocity associated with atmosphere probes of Jupiter, provided that no propulsive braking is utilized. Today's entry technology clearly does not permit such an entry and much work must be done if such a mission is to be attempted. Because Jupiter entry probes are so far in the future, no further consideration will be given to them here.

FLIGHT MECHANICS AND MOTION

Among the primary problems in flight mechanics and motion appropriate to entry vehicle technology are determination of the permissible entry corridor, range capability, the ability to deploy decelerators such as parachutes, and the ability to land horizontally. Each of these places certain requirements upon vehicles, and influences the reentry physics phenomena through their dependence upon both entry trajectory and vehicle configuration. The implications of these will be discussed for Earth and Mars entry.

Earth Entry

The entry corridor is defined for super-circular entry as the range of entry angle permitted to a vehicle between the boundaries representing skip-out (overshoot) and excessive deceleration (undershoot). The allowable corridor is frequently described by a linear dimension, the corridor depth, defined by Chapman (ref. 2) as equal to the difference in the vacuum perigees for the corresponding overshoot and undershoot trajectories. The corridor available to a vehicle depends upon the planet, its atmosphere, the entry velocity, and vehicle aerodynamic characteristics, and must be sufficiently deep to accommodate approach guidance tolerances.

A very thorough discussion of earth entry flight mechanics was given by Love (ref. 1). It was shown there that the available corridor decreased rapidly with increasing entry velocity, increased with increasing lift/drag ratio, and was further increased if the modulation of lift through vehicle attitude change was permitted. For entry velocities characteristic of return from a mission to Mars, these trends are graphically illustrated by Figure 2, a plot of available corridor depth as a function of maximum hypersonic lift/drag ratio for two velocities and two lift modulation schemes. These data are cross-plotted from the data of Pritchard (ref.3). For the roll-modulated case, the vehicle flies at a fixed

attitude corresponding to a fixed ratio of the resultant lift to drag; however, the vertical component of lift may be modulated through rolling the vehicle about the flight path axis. Lateral translation will result, but this may be compensated by later maneuvers, if desired. The entry through pullout is at maximum positive lift-to-drag ratio. For this case, the overshoot boundary is defined by the minimum entry angle permitting constant altitude flight with negative lift/drag ratio after pullout (i.e., the vehicle rolls 180 degrees at pullout), and the undershoot boundary is defined by a 12g limit on resultant deceleration.

Angle of attack changes are permitted in the pitch modulated case in addition to roll. For this case the overshoot criterion is the same as for the previous case, but the undershoot boundary is somewhat different. In undershoot, pitch modulation is employed when the 12g deceleration limit is reached such that this deceleration is maintained as the lift coefficient decreases through zero and to maximum negative L/D. Roll modulation at constant altitude is then assumed.

For the roll-modulated vehicle, large increases in maximum lift/drag ratio beyond a value of about one, offer only a small increase in available corridor depth. If the guidance accuracy is assumed to be typically about 15 km, the roll-modulated vehicle provides a sufficient corridor depth for L/D

greater than $1/2$ at 15.2 km/sec, typical of the entry velocities for return trajectories from Mars, but provides a maximum of only about 10 km at the extreme high energy return velocity of 21.3 km/sec. In contrast, the pitch-modulated vehicle not only provides sufficient corridor depth at $L/D=1$ for the higher velocity, but can more profitably employ higher L/D if required. The penalty one must pay for pitch modulation is in vehicle weight and complexity. Movable control surfaces will be required to provide pitch modulation, and these must project well into the high energy airstream to be effective, thus creating an aerodynamic heating problem of major proportions. In addition, undershoot entries are steeper for the pitch-modulated vehicle and higher radiative heating rates and loads are encountered compared to the roll-modulated vehicle of equal maximum L/D . However, for a given corridor depth, lower L/D is required for the pitch-modulated vehicle and this trend is reversed (see ref. 3).

The preceding discussion has shown a requirement for L/D ranging from about $1/2$ to 1 for earth return from Mars, depending upon return velocity and lift modulation scheme utilized. Vehicles providing such a capability will be necessarily relatively slender compared to today's operational manned entry vehicles. Such a family of vehicles is the so-called lifting body, with a lift/drag ratio ranging from

about $1/2$ in the blunter vehicles to about $1-1/2$ for the more slender vehicles (refs. 4 and 5). It will be shown later that the relatively slender vehicles are also compatible with requirements resulting from consideration of radiation heat transfer at hyperbolic velocities.

Once the requirement for hypersonic L/D of the order of one is established to meet entry corridor requirements, significant longitudinal and lateral range capability is afforded for selection of the landing point, and the possibility of having conventional landing capability is established. For the latter capability, a subsonic L/D of from three to five appears desirable, depending upon vehicle wing loading. Such a subsonic L/D appears feasible for a vehicle with hypersonic L/D of about one, and glide tests of a research entry vehicle of this type, shown in Figure 3, will soon begin at the NASA Flight Research Center.

Mars Entry

Many of the same considerations discussed for earth entry are of interest for entry into the atmosphere of Mars. In addition, the problem of ballistic entry of unmanned probes or landers and the complication of an uncertain atmospheric composition and structure are introduced. Estimates of the surface pressure at Mars, which had ranged from about 10 to 85 mb

in recent years, have been revised downward to more nearly 10 mb, based upon the results of the recent Mariner IV flyby. Atmosphere composition is still not established with any certainty. Definition of the atmosphere structure and composition with sufficient accuracy for detailed design of optimum vehicles may not be possible until direct measurements by unmanned probes or landers are made. Until that time, design of Mars entry vehicles will, of necessity, be sufficiently conservative to permit successful entry (and soft landing, if appropriate) for the range of likely atmospheres. Levin, Evans, and Stevens (ref. 6) provide a list of references proposing models of the Martian atmosphere and, corresponding to the recent measurements of Kaplan, et al, (ref. 7) and Kuiper (ref. 8), have generated three tentative engineering models useful for deceleration and heating calculations. The effect of Martian atmospheric uncertainties upon flight mechanics parameters will be discussed in the subsequent paragraphs.

Hyperbolic entry at Mars of ballistic vehicles is of interest in terms of unmanned atmosphere probes and landers. Because deceleration tolerances of instruments tend to be significantly greater than those of man, entry corridor considerations for such systems are not usually critical. However, to ensure landing at tolerable impact velocities,

such vehicles must decelerate sufficiently in the atmosphere to allow for the deployment of decelerators such as parachutes. If the atmosphere is as tenuous as suggested by Kaplan and Kuiper, as well as by the Mariner IV results, vehicles will have to be quite blunt and lightly loaded in order that deployment velocities are reached at sufficiently high altitude. The degree to which the atmosphere influences the vehicle design for this case may be seen from the following simple calculation.

The expression

$$V/V_E = e^{-(C_D A \rho H_p / 2m \sin \gamma_E)} \quad (1)$$

from ref. 9, defines the velocity of a ballistic entry vehicle during its entry for conditions of an isothermal atmosphere with constant density scale height H_p and decelerations large with respect to the local gravity. V is the velocity, V_E the entry velocity, $m/C_D A$ the ballistic parameter, ρ the ambient density, and γ_E the entry angle. The stratosphere of each of the three model atmospheres of reference 6 is isothermal and has an approximately constant density scale height. They have each been approximated by an idealized isothermal atmosphere, with the density relation

$$\rho/\rho_{ref} = e^{-(h/H_p)} \quad (2)$$

where h is the altitude, and the constants are as given in the table.

Model	1	2	3
$\rho_{\text{ref}} \text{ (gm/cm}^3\text{)}$	5.28×10^{-5}	5.69×10^{-5}	1.09×10^{-4}
$H_p \text{ (km)}$	20.9	14.0	6.5
Model Surface Pressure			
$p_0 \text{ (mb)}$	40	25	10
Idealized Surface Pressure			
$p_{\text{ref}} \text{ (mb)}$	39.6	28.6	25.4
Tropopause Altitude (km)	22	18	10

Thus, the idealized atmospheres are good fits to the respective models above the tropopause and equation (1) is approximately valid here.

Equations (1) and (2) may be solved for the altitude at which the velocity is reduced to a specified fraction of the entry velocity. This has been done for $V/V_E = 0.05$, corresponding to reasonable velocities for deployment of conventional parachutes and for vertical entry, and the results are plotted in Figure 4 as a function of $m/C_D A$ for each of the three idealized atmospheres. The dashed portion of the curves represent altitudes below the corresponding tropopause and the results are invalid here. If a minimum deployment altitude of about 10 km is assumed, the figure shows that values of the ballistic parameter somewhat greater than 6 gms/cm² are tolerable for Model 1, while a value of about 2.5, about as low as can be attained in practice, is required for Model 3.

Entry at some angle other than vertical would alleviate these results somewhat, but would still require low values of $m/C_D A$. Without better definition of the atmosphere, Model 3 would necessarily be the design model for parachute deployment, and would require extremely blunt, lightly loaded, entry vehicles. This restriction, coupled with the associated high levels of radiative heating, results in rather small payload to gross weight ratios. Related aspects of this problem were discussed by Roberts (ref. 10) and Seiff (ref. 11).

The aforementioned atmospheric uncertainties could have major impact on hyperbolic manned entry vehicles as well. Such entries would be appropriate if atmosphere braking were to be used either for direct landing on the planet surface from a hyperbolic approach trajectory or for capture of an approaching vehicle. The latter maneuver is part of a mission mode called Mars Orbit Rendezvous in which the mission vehicle enters hyperbolically, is decelerated aerodynamically to approximately circular satellite velocity, and then, through a maneuver utilizing lift, exits the atmosphere. When an appropriate altitude is reached, a moderate propulsive maneuver is used to establish an orbit. From this orbit, an excursion module may be dispatched to the surface and, upon return, rendezvous with the parent vehicle prior to departure

for Earth. In either case, direct entry or entry to orbit, atmosphere braking can be more efficient than the corresponding propulsion maneuver in terms of equivalent specific impulse, as is shown later.

For such hyperbolic entries, the concept of an entry corridor may be used to define lift requirements as a function of entry velocity and atmospheric characteristics. Consideration was given to such entry corridors by McKenzie (ref. 12) and Napolin and Mendez (ref. 13), and Figure 5, cross-plotted from McKenzie's data, illustrates the available corridor for atmospheres of two different scale heights within the range of the models of reference 6. In this figure, the lift/drag ratio is constant at $\pm 1/2$, undershoot is defined by a resultant deceleration of $10g$ with the lift vector directed outward, and overshoot by capture requirements with the lift vector directed towards the planet. As can be seen, if a guidance accuracy of 15 km is assumed, sufficient corridor would be provided even for the smaller value of scale height for the full range of velocities of interest. For a given scale height, surface pressure level is not a factor in determining available corridor because this pressure tends only to fix the altitude at which maneuvers take place. In the case of Figure 5, the minimum altitudes for undershoot are above surface level even for a surface pressure as low as 11 mb .

Atmospheric uncertainties introduce a more subtle effect in available corridor depth, however. Scale height, as well as surface pressure, influences the altitude at which the corridor is placed. Without precise determination of these parameters, an approaching vehicle would be limited to that corridor defined by the lowest overshoot boundary and the highest undershoot boundary appropriate for the range of postulated atmospheres. The curve labeled COMPOSITE in Figure 5 represents the result of this consideration as influenced only by scale height uncertainty in the range specified, and shows that for velocities above 9 km/sec in this case, the available corridor is decreased rapidly with increasing velocity and vanishes at about 10.5 km/sec. Consideration of a range of possible surface pressures would reduce the corridor still further. Clearly a vast improvement in our knowledge of the Martian atmosphere is important in order that the full benefits afforded by atmosphere braking can be realized. As for earth entry, increasing the lift/drag ratio and providing lift modulation capability both increase the available entry corridor and, for Mars, reduce the impact of atmospheric uncertainties.

The provision of lifting capability for hyperbolic Mars entry vehicles utilizing the Mars Orbit Rendezvous mode has an additional benefit, that of permitting plane change during

entry. Such a maneuver would allow greater flexibility in incoming trajectory parameters while still permitting post-entry orbits consistent with possible landing locations and subsequent desirable Mars escape trajectories. This aspect of atmosphere braking at Mars was considered by Napolin and Mendez (ref. 13), and Figure 6 herein displays a representative result. The plane change capability for an entry velocity of 8.4 km/sec is plotted against lift-to-drag ratio with undershoot defined by 5g resultant decelerations and overshoot by maintenance of level flight with maximum negative L/D (roll modulation). For an L/D of 1/2, a modest plane change of about 10 degrees is afforded, but for L/D of one, this capability has increased to about 25 degrees, permitting considerable flexibility in trajectory selection.

The entry velocities for a Mars excursion module capable of entry from an orbiting parent spacecraft are considerably lower than those appropriate to hyperbolic entry. One study of such a vehicle, described by Dixon (ref. 14), has determined that a half-cone vehicle with L/D of about one is feasible from a motion and heating point of view, with the heat protection afforded through reradiation. The lift capability of such a vehicle is particularly important for lateral range capability.

Entry flight mechanics, because they are not sensitive to atmosphere composition, are expected, for Venus entry, to be very much like those at Earth. For ballistic probes, the major problems are expected to be those related to entry heating at velocities greater than 11 km/sec in a possibly dense atmosphere with appreciable concentration of CO_2 .

FLOW FIELDS AND HEATING

It has been established from our considerations of flight mechanics and motion that relatively slender lifting vehicles are appropriate for hyperbolic entry at Earth and Mars for manned vehicles, and that extremely blunt ballistic probes appear to be required for unmanned Mars landers. A brief summary of the problems and progress in understanding flow fields and heating of such vehicles is now given. Except where noted, the discussion is limited to a reacting gas mixture in chemical equilibrium because, in general, non-equilibrium effects on radiative and convective heating have been shown to be of less over-all importance (e.g., ref. 15).

Inviscid, Adiabatic Shock Layer

Although for earth entry at velocities much above parabolic the effects of shock layer radiation and conduction are important in the determination of shock layer structure, it is

instructive to consider the inviscid, adiabatic shock layer both for direct application at lower velocities and for comparison with shock layers determined including these energy transfer mechanisms at the high velocities. Seiff (ref. 16) reviewed the status of flow field analysis in 1962. Since that time, further advances have been accomplished, including the further development of two methods which appear capable of analyzing the flow about a blunt nose at large angle of attack. The first method, a direct, essentially exact numerical method, avoids the usual complexity of attempting to integrate the elliptic equations in the subsonic portion of the flow field by treating the problem as one in unsteady aerodynamics. The unsteady equations are hyperbolic with well defined initial conditions and can be integrated to arbitrarily large times such that the steady state flow is approached as closely as desired. Such a method is that of Bohachevsky, Rubin, and Mates (ref. 17). Further development of this approach should make possible the treatment of the flow about arbitrary bodies with realistic high temperature gas properties.

The second method discussed here is the approximate method of Kaattari (ref. 18) in which mass flow continuity in the shock layer and empirical correlations were used to define the shock shape and shock layer properties for blunt

bodies at large angles of attack. The method is appropriate for flow of an ideal gas or reacting gas mixtures at equilibrium. Some interesting results were given by Katzen and Kaattari (ref. 19) and are reproduced here as Figures 7 and 8. It was determined that stagnation point shock stand-off distance for equilibrium flow could be correlated as a function of normal shock density ratio for a fixed geometry. The curves of Figure 7 show such correlations for spherically blunted cylinders of various nose radii as derived by Katzen and Kaattari. Also shown for a hemisphere-cylinder is the stand-off distance correlation derived by Lomax and Inouye (ref. 20) by an inverse method. Agreement of the two methods is good. Except for the recent work of Bohachevsky, et al., this family of shapes (other than the hemisphere-cylinder) has not been amenable to calculation before.

Shock shapes for a flat-faced cylinder at angle of attack are shown in Figure 8(a) and compared to experimental data at 30 degrees angle of attack for a density ratio of 0.25. Pressure distribution for the same shape is compared to experiment at 20 degrees angle of attack in Figure 8(b). In both cases, agreement between experiment and prediction is extremely good, and this method should prove extremely versatile. It has also been extended successfully to the

calculation of stand-off distance for nonequilibrium flows and for flows with gases injected into the shock layer (ref. 19).

Convective Heat Transfer

Any discussion of the laminar heat transfer in air at hyperbolic velocities must begin with consideration of the transport properties of ionized air. Predictions of stagnation point heat transfer to date have been based on transport properties predicted by simplifications of the Chapman-Enskog formulation (see refs. 21 and 22). Typical of such calculations are those of ref. 23 based upon the transport properties of Hansen (ref. 24). While agreement between heat transfer prediction and experiment has been satisfactory up to equivalent flight velocities of about 15 km/sec, corresponding to about 50 percent ionization of air, we realize now that this is a result of the relative insensitivity of surface heat transfer rate to thermal conductivity outside the boundary layer. Figure 9, a plot of total thermal conductivity as a function of temperature, was used by Ahtye (ref. 22) to demonstrate the inability of the simplified theory to predict the experimentally observed values of Maecker (ref. 25) for nitrogen when ionization becomes important. Ahtye has utilized the rigorous second order theory for partially ionized

argon in references 21 and 22, and these results should give some indication of the importance of the previously neglected effects in more complex gases. An example of this effect is given in Figure 10, wherein the translational thermal conductivity is plotted as a function of temperature, at a pressure of 10^{-1} atm, for both the simplified and more rigorous second order theories. The latter values are greater by some 30 to 50 percent when ionization is appreciable.

Heat transfer for equilibrium mixtures depends upon reactive and thermal diffusive components of conductivity, as well as on the translational component. The first two components are dependent upon multi-component and thermal diffusion coefficients. These coefficients have been calculated for partially ionized argon by Ahtye (ref. 22). However, the reactive and thermal diffusive components depend also upon macroscopic concentration gradients for ions and electrons and the charge-separation field which may affect these gradients. These effects have not yet been determined, and thus the accurate prediction of convective heat transfer in highly ionized gases is not yet possible.

Some indication of how important an order of magnitude change in total thermal conductivity might be to convective heat transfer in air is given by Figures 11 and 12, from Howe and Sheaffer (ref. 26). Figure 11 shows assumed thermal

conductivity curves (and Maecker's data) as a function of temperature. Curve I is the prediction of Yos (ref. 27) which fits the data quite well until ionization becomes important; curve II corresponds to an arbitrary increase of roughly an order of magnitude over Yos' curve in the region of important ionization; and curve III approximates the prediction of Hansen up to 15,000°K and then is faired into the Yos curve. Stagnation point heating rates were calculated by Howe and Sheaffer for each of these assumed conductivity functions and the results are shown in Figure 12. Although these values were calculated for a viscous, conducting shock layer with radiation transfer, the Reynolds numbers are sufficiently high and the radiant transfer sufficiently low that the results correspond closely to a more classical boundary layer calculation. It is evident that the order of magnitude difference in conductivity appears as only a factor of two in heat transfer rate at the highest enthalpy level shown, and then only for equivalent velocities greater than about 20 km/sec. Shown also is the prediction of Howe and Viegas (ref. 28) wherein Hansen's properties (to 15,000°K) were used. If this is extrapolated linearly to higher velocity, it lies roughly halfway between the two extremes shown. Because experiments have been limited to conditions corresponding to a maximum of about 15 km/sec, the reason that no discrepancies between experiment and theory have been noted, even with

50 percent ionization, is the relative insensitivity of heat transfer to thermal conductivity external to the boundary layer for these velocities. It is evident that, should the second order total conductivity predictions, when established, show even an order of magnitude increase over the current approximations above 10,000°K, experiments at equivalent velocities greater than 20 km/sec will be required to confirm the effect upon heat transfer rate. Nevertheless, such velocities are at the upper end of those appropriate for direct return from Mars, and these effects may well have an important influence on vehicle selection and design.

The relative insensitivity of heat transfer to high temperature gas properties for relatively cold walls was shown by Marvin (ref. 29) for various other pure gases at velocities up to about 10 km/sec. It was found that a single correlation could be established for all the gases considered (CO_2 , Air, N_2 , H_2 , A) in terms of low temperature transport properties. These results are shown in Figure 13, wherein all the numerical results are within ± 16 percent of the correlation function. Plotted is a convective heat transfer parameter against enthalpy ratio. ϕ_D is the ratio of density-viscosity product at the onset of dissociation (or ionization in the case of argon) to that at the wall, h_D is

the corresponding static enthalpy, and g is the ratio of total enthalpy to that outside the boundary layer. Marvin also found that the laminar heating rate distribution to blunt bodies, as calculated from local similarity principles, was little affected by composition, and, as for air, can be obtained with reasonable accuracy from the inviscid flow alone so long as the pressure gradients are not too large (ref. 30) and from ideal gas boundary layer solutions when pressure gradients are high (ref. 31).

Unfortunately, our understanding of transition and turbulent heat transfer at reentry velocities has not advanced to the same degree as has that for laminar flow in the past few years. The mechanisms leading to transition are not well defined and hence theoretical predictions can not be derived. Empirical transition criteria have been derived from low velocity ground facility and small scale flight experiments, but how they can be extrapolated to flight conditions at moderate to high local Mach numbers, small ratios of wall to total enthalpy, and in the presence of ablation, has not yet been well established. Much the same situation holds for turbulent flow at reentry flight conditions. Turbulent skin friction and heating predictions are also based upon relatively low velocity data with corrections for high temperatures, enthalpy ratios, and Mach number through a variety of estimation techniques (see refs. 32 and 33). One can show that a requirement for a significant increase in

our ability to predict transition and turbulent flow phenomena exists for the hyperbolic lifting entry vehicles appropriate for future missions. For example, typical boundary trajectories for earth entry at velocities appropriate to return from Mars are shown on an altitude-velocity plot on Figure 14. The vehicle is assumed to have a maximum L/D of one with modulation by roll control, a ballistic parameter ($m/C_D A$) of 49 gm/cm^2 , and enters at a velocity of 15.2 km/sec . Plotted also are lines of constant free-stream Reynolds number based on a length of 10 meters, typical of the over-all length of contemplated vehicles. The vehicle would experience maximum free-stream Reynolds numbers of about 3×10^6 based upon vehicle length during the undershoot trajectory; local Reynolds numbers based upon conditions outside the boundary layer and the length of the vehicle would be roughly an order of magnitude lower, or of the order of 10^5 . Reynolds numbers based upon local conditions and laminar momentum thickness would be roughly 500. Each of these values is sufficiently large that transition must be considered a distinct possibility, particularly in the presence of the mass transfer and surface roughness associated with ablation.

Radiative Heating

It has become apparent in the past few years that as contemplated entry velocities were increased above parabolic escape

speed at Earth, the contribution of radiative energy transfer from the hot shock layer would have to be considered in vehicle design along with that from conduction in the boundary layer. In fact, for very blunt vehicles (as appropriate to satellite reentry and lunar return) the radiative input would dominate even for velocities at the lower end of the Mars return velocity spectrum. Detailed consideration of both mechanisms of energy transport has led to the concept of more slender vehicles to compensate for the potentially dominant radiative transfer; these will be described in a subsequent section. In this section, some recent radiative research results will be briefly discussed.

The principal radiators and the corresponding radiative intensities for high temperature air and gases thought to be representative of the atmospheres of Mars and Venus are reasonably well established for conditions corresponding to velocities up to approximately 8 km/sec. In this flight regime, the dominant radiation sources are molecules undergoing radiative transitions from excited states to states of lower energy. Some recent data obtained in a free flight facility by Arnold, Reis, and Woodward (ref. 34) for mixtures of CO_2 and N_2 are shown in Figure 15. These data are appropriate for flow fields in chemical equilibrium and the emission is seen to correlate with a function of density and velocity in much the same manner as does that for dissociated air. Shown also

is the prediction for air of Kivel and Bailey (ref. 35) and it is apparent that at the lower velocities radiation from the $\text{CO}_2\text{-N}_2$ mixture exceeds that for air by as much as an order of magnitude. This effect is attributed to the radiation from the CN-violet band system which dominates the emission for the former case. Other shock tube and free flight data and predictions (refs. 36, 37 and 38) are shown in the figure as indicated. At velocities above about 10 km/sec, radiation resulting from recombination of ions and electrons, bremsstrahlung, and atomic line radiation become the dominant factors, and in this region the $\text{CO}_2\text{-N}_2$ mixtures and air behave in a similar manner. This is expected since few molecules exist at the correspondingly high temperatures (about 10,000°K and above).

Not properly accounted for in this work is the increasingly important contribution to the continuum radiation of sources at wavelengths shorter than 2000 Å for air and $\text{CO}_2\text{-N}_2$ mixtures. Recent work by Biberman, et al., (ref. 39), Nardone, et al., (ref. 40) and Hahne (ref. 41) has demonstrated the importance of this region of the spectrum for velocities much above 10 km/sec. The intensity of this radiation is such that the radiating gas layer must be treated as self-absorbing for these wavelengths, complicating the heretofore conceptually simple scaling relations. The impact of this recent work is yet to be fully determined.

Although the simple model of an adiabatic, optically-thin shock layer has been generally appropriate for the calculation of radiation heat transfer to vehicles of moderate size entering planetary atmospheres at velocities up to about 15 km/sec (provided the vacuum ultraviolet contribution is not considered), higher velocity applications require that the effects of energy transfer, both by radiation and conduction, be considered in determining the shock layer. Wilson and Hoshizaki considered the effect of large radiation transfer upon the inviscid flow field of hemisphere-shaped bodies by an integral method (ref. 42), and determined the resulting radiation relative to that for an assumed adiabatic shock layer. The gas was considered optically thin. For the stagnation point flow, the radiation was found to decrease significantly when the energy radiated from a mass of gas traversing the stagnation region (as calculated for adiabatic flow) became as large as the order of 1/10 of its initial total energy. This is shown in Figure 16. Plotted is the ratio of radiation transfer for the non-adiabatic case to that for adiabatic flow as a function of an energy loss parameter, defined as the ratio of radiation emitted for adiabatic conditions to total flow energy. The radiant heat transfer distribution about the hemisphere was found to be essentially the same as for the adiabatic case, if plotted in terms of the ratio of local to corresponding stagnation value.

Both Howe and Viegas (ref. 28) and Hoshizaki and Wilson (ref. 43) analyzed the radiating viscous shock layer. In the former, only the stagnation region was considered for a grey gas. It was found that the convective heat transfer was significantly reduced for cases where radiant heat transfer caused the enthalpy outside the edge of the viscous layer to be reduced, although a simple correlation in these terms was not possible. These results are plotted in Figure 17 at one atmosphere pressure and for various nose radii. Because of the relatively strong dependence of radiation upon gas density, the decrease in the convective heating parameter would be greater for higher pressures. The effect of radiation cooling on the radiant heat transfer itself was found to be essentially independent of the inclusion of heat conduction (for the Reynolds numbers considered), and the results are in agreement with those of Wilson and Hoshizaki, as shown in Figure 16.

Hoshizaki and Wilson (ref. 43) retained the optically thin assumption in extending the integral method to the viscous shock layer. Two different estimates of the emissivity of air were used, one corresponding to the estimates of Meyerott, et al. (ref. 44), and the other to the somewhat higher estimates of Kivel and Bailey (ref. 35). For the stagnation point, the results were found to be in general agreement with those of Howe and Viegas. Distribution of

both convective and radiative heat transfer rates about a hemisphere were again found to be roughly independent of the level of radiation, provided they were plotted in terms of the ratio of local to corresponding stagnation point values. These results are shown in Figures 18(a) and 18(b). Note, however, that the level of heating, both convective and radiative, depended upon the magnitude of the radiation transfer.

The influence of the intense radiation in the vacuum ultraviolet upon these results must now be determined. One cannot say a priori that the stagnation point correlation of Figure 16 and the invariance of distribution with radiation cooling level, as shown in Figures 18(a) and 18(b), will remain unchanged because self-absorption of the UV radiation will tend to influence the convective heat transfer through heating of the gas adjacent to the surface, and the influence may be a function of local conditions on the body. This should be a fruitful area of investigation.

VEHICLE CONFIGURATION ASPECTS

The performance of heat protection systems, whether operating by ablation, reradiation, transpiration, film cooling, or simply by energy storage, must be determined along

with the flow field and energy transfer characteristics external to the vehicle in order that efficient vehicle concepts be derived. Reradiative systems are appropriate, with the present high temperature materials technology, to the low levels of heating sustained over long durations, such as for lifting vehicles ($L/D \approx 2$ or more) entering the Earth's atmosphere at satellite velocity. For higher velocities, or when heating pulses are of large magnitude and short duration, ablation, transpiration, or film cooling systems are more appropriate, with ablation having been used almost exclusively in recent years. The inefficient heat sink type of system is generally not competitive except perhaps for special applications.

Heat protection system performance per se will not be discussed here in any detail; rather, some simple models of ablation will be used to demonstrate the importance of the convective and radiative heating inputs upon vehicle configuration for super-satellite entry velocities at Earth.

The apparent dominance of radiative heating over convective heating for blunt bodies at velocities greater than parabolic escape speed at Earth (for example, refs. 45 and 46), has led to the study of moderately slender cones with a pointed rather than a blunt nose for such reentry conditions. Allen, Seiff, and Winovich (ref. 15) analyzed a family of

such cones for hypervelocity ballistic earth entry and some pertinent results are shown here. Two ablators were considered, one a low temperature ablator having the assumed characteristics of subliming teflon, and the other a high temperature ablator having the assumed characteristics of vaporizing quartz. The cone was assumed to remain sharp; the details of the analysis are given in the reference. In the analysis, optimum cone angles were computed for minimum absorbed energy fraction as a function of entry velocity for both all-laminar and all-turbulent flow. The results for laminar flow, both with the teflon and quartz ablators, are shown in Figure 19. Corresponding results for turbulent flow are shown in Figure 20. In these figures, η is the absorbed energy fraction (ratio of absorbed energy to initial kinetic energy) and θ_c is the semi-vertex angle of the cone. The parameter B is a ballistic parameter defined by

$$B = \frac{C_D A}{m} \frac{\rho_0 H_p}{\sin \gamma_E}$$

where ρ_0 is the atmospheric density at the surface and the other parameters are as defined previously.

One important point to note from these results is that for each optimum condition, convection contributes approximately 85 to 90 percent of the total energy absorbed, and for the radiative models used, equilibrium radiation accounts for

most of the balance (nonequilibrium radiation input is generally negligible). At first glance, this behavior appears somewhat anomalous when the tendency towards dominance of radiative transfer over convective transfer at such velocities is considered. For stagnation flows, for example, optimum nose radii were calculated for minimum energy transfer by Howe and Sheaffer (ref. 47) and for these cases, radiation transfer exceeded net convective transfer by factors of from two to nine. No real anomaly exists, however; for given flows over sharp cones, convection decreases slowly and radiation increases rapidly with increasing cone angle, while for increasing nose radius in stagnation flow, convection decreases almost as rapidly as radiation increases. As a result, the optima are shifted with respect to one another. In either case, for a given configuration (cone angle or nose radius) radiation would tend towards dominance for velocities greater than that corresponding to the optimum. Note also that reference 15 considered total energy transfer while reference 47 calculated minimum heating rate.

Optimum cone semi-vertex angles tend to be rather large, from 25 to 50 degrees, for the range of parameters shown, both

for laminar and turbulent flow. For turbulent flow, the absorbed energy fractions are nearly an order of magnitude greater than for laminar flow, a result of the aforementioned dominance of the convective energy absorbed. This result is graphically illustrated in Figure 21, a plot of laminar and turbulent optimum energy fractions as a function of ballistic parameter for various entry velocities. The laminar curves are assumed valid for local Reynolds numbers less than 10^7 , and the dashed portions of the curves represent arbitrary fairings to join with the turbulent curves. One can conclude that important areas for future research should be those associated with determination of transition criteria, maintenance of laminar flow, and determination with greater confidence of the turbulent heating levels for reentry conditions.

The analysis described above neglected the effect of shape change. If shape change were permitted, the sharp cones would rapidly blunt, radiative transfer would be much enhanced in the nose region, and the resulting surface recession in the nose regions would tend to continually accelerate the blunting effect during an entry. This suggests that some means of providing nonablative tips should be sought. Transpiration or film cooling may be appropriate means of providing such protection. Such nonablative heat protection

techniques may also be desirable for entry vehicles which are designed for re-use.

The results just described were derived specifically for ballistic entry. No equivalent parametric analysis has been performed for lifting entry; such an analysis would be much more complex. However, a conceptual lifting entry vehicle design study for one set of entry conditions was carried out and is reported by Hearne, Chin, and Lefferdo (ref. 48). The vehicle configuration consisted of a spherically-blunted circular cone aligned with its axis parallel to the direction of flight, and with its base raked off at an angle to provide the desired lift. An elliptic cone afterbody was fitted to the raked-off base to provide useful volume. The vehicle studied had a lift/drag ratio of 0.6, and a ballistic parameter ($m/C_D A$) of about 100 gm/cm^2 . For given gross weight and volume (including afterbody), a cone semi-vertex angle of about 40 degrees was found to yield minimum heat shield weight for entry into the Earth's atmosphere at 19.8 km/sec with a phenolic-nylon ablative heat shield assumed.

Two levels of radiative heating were assumed; the large (nominal) corresponding roughly to the estimates of Nardone, et al. (ref. 40), and the smaller equal to 1/10 that amount. Heat shield mass is plotted for each case as a function of

cone angle for these two estimates in Figure 22. For the larger emission, the optimum angle is about 43 degrees, and when the radiative input is reduced an order of magnitude, the optimum shifts to an angle above 45 degrees while the heat shield mass is reduced to a value estimated to be about one-half that for nominal emission. The fact that the heat shield masses are not in proportion to the emission levels is attributed to the influence of convective heating, radiative cooling of the shock layer, reradiation from the heat shield surface, and the presence of unaffected heat shield insulation.

The effect of transition Reynolds number is shown in Figure 23, a plot of heat shield mass against cone angle for three values of transition Reynolds number based upon momentum thickness. As expected, an increase in transition Reynolds number results in a decreased optimum cone angle and a total heat shield mass reduction of a factor of about two for the values shown. This again demonstrates the importance of the determination of transition criteria and turbulent heat transfer.

RELATIVE MERITS OF AERODYNAMIC AND PROPULSIVE BRAKING

Allen (ref. 49) considered the relative merits of propulsive and aerodynamic braking for deceleration at earth return. This comparison was based upon the results for ballistic entry

of sharp, ablating cones described previously (ref. 15). Plotted in Figure 24 is the equivalent specific impulse for the teflon and quartz ablators as a function of entry velocity, for laminar flow. Shown also are typical specific impulse values appropriate to chemical and nuclear rockets. Equivalent specific impulse values for the aerodynamic braking case with turbulent flow would be about one order of magnitude lower than for laminar flow, and for teflon would be of the same order as the propulsion systems, while quartz would still be more effective. More complete comparisons making use of estimated engine, propellant tank, and structure weights for propulsive systems, and insulation and structure weights for atmosphere braking systems, should be investigated. So long as laminar flow can be maintained, however, it is expected that the advantage would remain with atmosphere braking.

Much the same advantage was shown by Tauber and Seiff (ref. 50) for atmosphere braking from hyperbolic approach velocities to orbital velocity at Mars, compared to the equivalent propulsive maneuver. In the reference, initial mass required in earth orbit to launch the missions was considered the measure by which relative advantage was determined, and systems utilizing rocket propulsion at Mars to perform the capture maneuver were approximately twice as

massive as those utilizing atmosphere braking. Thus atmosphere braking to orbit at Mars for manned missions appears to offer a significant advantage over propulsive braking from a vehicle weight standpoint. Its ultimate selection, however, will depend upon many factors, such as the level of heat shielding technology, ability to store and insulate cryogenic fluids from the entry heating loads, and residual uncertainties in the Martian atmosphere.

GROUND SIMULATION AND FACILITIES

Ground facilities capable of simulation of one or more of the parameters characteristic of reentry flight have advanced considerably in the past few years. Although the shock tube will continue as the primary tool for the determination of high temperature properties of gases and for measurements of phenomena which are essentially independent of free stream simulation, such as convective heat transfer to the forebody of blunt configurations, new facility concepts which hold much promise have been or are being developed.

For the simulation of free stream velocity, Mach number, and Reynolds number, extensive development of ballistic shock tunnels has been pursued. In this type of facility, a small model is fired from a light gas gun into a countercurrent

gas stream generated by a shock tunnel. Relative velocities of about 13 km/sec have been attained with models of about 1/2 cm diameter (ref. 51).

Roughly similar capabilities with a model fixed relative to the laboratory should be possible with a new concept, the expansion tunnel (ref. 52). The tunnel is essentially a double diaphragm shock tube with the cross-sectional area increased downstream of the second diaphragm. The test gas is placed between the two diaphragms and is first compressed and accelerated by the shock wave generated through rupture of the first diaphragm. This gas subsequently undergoes expansion and further acceleration by both the unsteady expansion wave generated by rupture of the second diaphragm and the steady expansion as it passes through the region of increasing area. The gas, by this time at low temperature and high velocity, then passes over the fixed, instrumented model. The expansion tunnel is a modification of an earlier concept, the expansion tube (ref. 53), with potentially greater utility.

Neither of the aforementioned types of facilities is capable of providing sufficiently long test times for research with high-temperature charring ablaters, and most work of this type has been carried out in various arc-heated wind tunnels. The recently developed constricted arc tunnel

(ref. 54) has been operated at enthalpies up to about 24×10^3 cal/gm, corresponding to a velocity of 14 km/sec, and may be appropriate for development of such ablation materials suitable for the next generation of entry vehicles.

The simultaneous attainment of reentry flight velocity, Mach number, Reynolds number, and heating history in ground facilities does not appear possible at this time. Investigation of these phenomena, shown to be important in the previous discussion, will have to be carried on with partial simulation, as in the past, and supplemented with well chosen reentry flight tests.

CONCLUDING REMARKS

Some recent advances in atmosphere entry have been reviewed against a background of the requirements of missions of the future. The requirements of unmanned and manned Mars missions have been emphasized, but some brief consideration was given to unmanned Venus and Jupiter missions and to manned near-earth missions.

Although the entry velocities characteristic of Mars entries are low by earth entry standards, problems somewhat different will be experienced. Unmanned ballistic probes must be of extremely high drag in order that they can

decelerate to sufficiently low velocities for parachute deployment. Thus, the blunt entry configuration is still of pertinence. Manned entry vehicles for both Mars and earth entry, on the other hand, may well tend to the less blunt configurations compatible with lift/drag ratios of the order of one and reduced radiative heating. The current uncertainty in the definition of the Martian atmosphere has serious implications for both unmanned and manned entry at Mars.

The prediction of laminar convective heat transfer and radiative heat transfer for velocities up to those corresponding to dissociation of molecules appears to be well in hand. The prediction of transition and turbulent heat transfer for high reentry velocities and the prediction of laminar convective and radiative heating at velocities inducing significant ionization is, at present, unsatisfactory. Critical to the improved prediction of laminar convective and radiative heating are the determination of second and higher order effects in thermal conductivity and the effects of radiation in the vacuum ultraviolet portion of the spectrum, respectively.

Finally, it is instructive to compare some of the conclusions reached in a review of atmosphere entry technology presented in 1961 (ref. 5) with those of the present paper.

In the previous review, the tendency of radiation heating to dominate the heating problem during hyperbolic entry was cited as a potential major problem, and this tendency still exists today. However, it has been determined during the intervening period that nonequilibrium radiation is not a major factor at high super-satellite velocities, and that radiative cooling alleviates, to a degree, the tendency of equilibrium radiation to dominate the convective heat transfer. Radiation in the extreme ultraviolet portion of the spectrum, not previously considered, has now been determined to be of major importance. However, self-absorption of this emission may tend to reduce the impact of this component of the radiation.

The situation with regard to transition and turbulent heating remains little changed from 1961. Of particular importance is the consideration of transition, because large lifting and nonlifting vehicles experience rather large Reynolds numbers during atmosphere entry. The existence of extensive regions of turbulent flow has been shown to result in an increase of an order of magnitude in heat protection requirements for a class of conical, ballistic, ablating configurations.

REFERENCES

1. Love, Eugene S.: Factors Influencing Configuration and Performance of Multipurpose Manned Entry Vehicles. J. Spacecraft Rockets, vol. 1, no. 1, Jan.-Feb. 1964, pp. 3-12.
2. Chapman, Dean R.: An Analysis of the Corridor and Guidance Requirements for Supercircular Entry into Planetary Atmospheres. NASA TR R-55, 1960.
3. Pritchard, E. Brian: Velocity Requirements and Re-Entry Flight Mechanics for Manned Mars Missions. J. Spacecraft Rockets, vol. 1, no. 6, Nov.-Dec. 1964, pp. 605-610.
4. Eggers, A. J., Jr.: The Possibility of a Safe Landing. Space Technology, Edited by Howard Seifert, John Wiley and Sons, Inc., 1959.
5. Eggers, A. J., Jr., and Wong, T. J.: Motion and Heating of Lifting Vehicles During Atmosphere Entry. ARS Journal, vol. 31, no. 10, October 1961, pp. 1364-1375.
6. Levin, George M., Evans, Dallas E., and Stevens, Victor, ed.: NASA Engineering Models of the Mars Atmosphere for Entry Vehicle Design. NASA TN D-2525, 1964.
7. Kaplan, Lewis D., Munch, Guido, and Spinrad, Hyron: An Analysis of the Spectrum of Mars. Astrophys. J., vol. 139, no. 1, Jan. 1964.
8. Kuiper, Gerard P.: Fifth Semiannual Status Report to National Aeronautics and Space Administration Lunar and Planetary Laboratory, University of Arizona Research Grant No. Nsg 161-61, Dec. 1963.
9. Allen, H. Julian, and Eggers, A. J., Jr.: A Study of the Motion and Aerodynamic Heating of Ballistic Missiles Entering the Earth's Atmosphere at High Supersonic Speeds. NACA Rept. 1381, (Supersedes NACA TN 4047).

10. Roberts, Leonard: Entry into Planetary Atmospheres. Aeronautics and Astronautics, Oct. 1964, pp. 22-29.
11. Seiff, Alvin: Developments in Entry Vehicle Technology. Presented at the AIAA First Annual Meeting and Technical Display, June 29-July 2, 1964, Washington, D.C.
12. McKenzie, Robert L.: Some Effects of Uncertainties in Atmosphere Structure and Chemical Composition on Entry into Mars. NASA TN D-2584, 1965.
13. Napolin, A. L., and Mendez, J. C.: Target Orbit Selection for Mars Missions Using Aerodynamic Maneuvering. Presented at the AIAA Aerospace Sciences Meeting, Jan. 20-22, 1964, New York, N.Y., (AIAA Preprint No. 64-14).
14. Dixon, Franklin P.: An Early Manned Mars Landing Mission Using the Mars Excursion Module. Presented at the NASA/AIAA Third Manned Space Flight Conference, Nov. 4-6, 1964, Houston, Texas.
15. Allen, H. Julian, Seiff, Alvin, and Winovich, Warren: Aerodynamic Heating of Conical Entry Vehicles at Speeds in Excess of Earth Parabolic Speed. NASA TR R-185, 1963.
16. Seiff, Alvin: Recent Information on Hypersonic Flow Fields. Proc. NASA-University Conference on the Science and Technology of Space Exploration, vol. 2, no. 55, NASA SP-11, 1962, pp. 269-282.
17. Bohachevsky, Ihor O., Rubin, Ephraim L., and Mates, Robert E.: A Direct Method for Computation of Nonequilibrium Flows with Detached Shock Waves. Presented at the AIAA Second Aerospace Sciences Meeting, Jan. 25-27, 1965, New York, N.Y., (AIAA Paper No. 65-24).
18. Kaattari, George E.: Shock Envelopes of Blunt Bodies at Large Angles of Attack. NASA TN D-1980, 1963.
19. Katzen, Elliott D., and Kaattari, George E.: Flow Around Blunt Bodies Including Effects of High Angles of Attack, Nonequilibrium Flow, and Vapor Injection. Presented at the AIAA Entry Technology Conference, Oct. 12-14, 1964, Williamsburg, Va., (AIAA Publication CP-9, pp. 106-117).

20. Lomax, Harvard, and Inouye, Mamoru: Numerical Analysis of Flow Properties About Blunt Bodies Moving at Supersonic Speeds in an Equilibrium Gas. NASA TR R-204, 1964.
21. Ahtye, Warren F.: A Critical Evaluation of Methods for Calculating Transport Coefficients of a Partially Ionized Gas. Proc. 1964 Heat Transfer and Fluid Mechanics Institute, Stanford Univ. Press, 1964, pp. 211-225.
22. Ahtye, Warren F.: A Critical Evaluation of Methods for Calculating Transport Coefficients of Partially and Fully Ionized Gases. NASA TN D-2611, 1965.
23. Cohen, Nathaniel B.: Boundary-Layer Similar Solutions and Correlation Equations for Laminar Heat-Transfer Distribution in Equilibrium Air at Velocities up to 41,000 Feet/Second. NASA TR R-118, 1961.
24. Hansen, C. Frederick: Approximations for the Thermodynamic and Transport Properties of High-Temperature Air. NASA TR R-50, 1959.
25. Maecker, H.: The Properties of Nitrogen to 15,000°K. Presented at Meeting on Properties of Gases at High Temperature, AGARD, Aachen, Sept. 21-23, 1959. AGARD Rept. 324.
26. Howe, John T., and Sheaffer, Yvonne S.: Effects of Uncertainties in the Thermal Conductivity of Air on Convective Heat Transfer for Stagnation Temperature up to 30,000°K. NASA TN D-2678, 1965.
27. Yos, Jerrold M.: Transport Properties of Nitrogen, Hydrogen, Oxygen, and Air to 30,000°K. Avco Rept. RAD TM-63-7, 1963.
28. Howe, John T., and Viegas, John R.: Solutions of the Ionized Radiating Shock Layer, Including Reabsorption and Foreign Species Effects, and Stagnation Region Heat Transfer. NASA TR R-159, 1963.
29. Marvin, Joseph G., and Deiwert, George S.: Convective Heat Transfer in Planetary Gases. Prospective NASA TR R-224, 1965.

30. Lees, Lester: Laminar Heat Transfer Over Blunt-Nose Bodies at Hypersonic Flight Speeds. Jet Propulsion, vol. 26, no. 4, April, 1956, pp. 259-269, 274.
31. Beckwith, Ivan E., and Cohen, Nathaniel B.: Application of Similar Solutions to Calculation of Laminar Heat Transfer on Bodies with Yaw and Large Pressure Gradient in High-Speed Flow. NASA TN D-625, 1961.
32. Spalding, D. B., and Chi, S. W.: The Drag of a Compressible Turbulent Boundary Layer on a Smooth Flat Plate with and without Heat Transfer. J. Fluid Mech., vol. 18, Part I, Jan. 1964, pp. 117-143.
33. Bertram, Mitchel H., and Neal, Luther, Jr.: Recent Experiments in Hypersonic Turbulent Boundary Layers. Presented at the AGARD Specialists Meeting on Recent Developments in Boundary-Layer Research, May 10-14, 1965, Naples, Italy.
34. Arnold, James O., Reis, Victor H., and Woodward, Henry T.: Theoretical and Experimental Studies of Equilibrium and Nonequilibrium Radiation to Bodies Entering Postulated Martian and Venusian Atmospheres at High Speeds. Presented at the AIAA Second Aerospace Sciences Meeting, Jan. 25-27, 1965, New York, N.Y., (AIAA Paper No. 65-116).
35. Kivel, B., and Bailey, K.: Tables of Radiation from High Temperature Air. AVCO-Everett Res. Lab. Res. Rept. 21, Dec. 1957.
36. James, Carlton S.: Experimental Study of Radiative Transport from Hot Gases Simulating in Composition the Atmospheres of Mars and Venus. AIAA Journal, vol. 2, no. 3, March 1964, pp. 470-475.
37. Gruszczynski, J. S., and Warren, W. R., Jr.: Experimental Heat-Transfer Studies of Hypervelocity Flight in Planetary Atmospheres. AIAA Journal, vol. 2, no. 9, Sept. 1964, pp. 1542-50.
38. Thomas, G. M., and Menard, W. A.: Experimental Measurements of Nonequilibrium and Equilibrium Radiation from Planetary Atmospheres. Presented at the AIAA Entry Technology Conference, Oct. 12-14, 1964, Williamsburg, Virginia, (AIAA Publication CP-9, pp. 170-185).

39. Biberman, L. M., Iakubov, I. T., Norman, G.E., and Vorobyov, V. S.: Radiation Heating Under Hypersonic Flow. *Astronautica Acta*, vol. X/Fasc. 3-4, 1964, pp. 238-252.
40. Nardone, M. C., Breene, R. G., Zeldin, S.S., and Riethof, T. R.: Radiance of Species in High Temperature Air. General Electric Co., Space Sciences Lab. Rept. R 63 SD3, June 1963.
41. Hahne, Gerhard E.: The Vacuum Ultraviolet Radiation from N^+ - and O^+ -Electron Recombination in High-Temperature Air. Prospective NASA TN D-2794, 1965.
42. Wilson, K. H., and Hoshizaki, H.: Inviscid, Nonadiabatic Flow About Blunt Bodies. Presented at the AIAA Aerospace Sciences Meeting, Jan. 20-22, 1964, (AIAA Preprint No. 64-70).
43. Hoshizaki, H., and Wilson, K. H.: The Viscous, Radiating Shock Layer About a Blunt Body. Presented at the AIAA Entry Technology Conference, Oct. 12-14, 1964, Williamsburg, Va., (AIAA Publication CP-9, pp. 65-76).
44. Meyerott, R. E., et al.: Absorption Coefficients of Air. AFCLRL, Geophysics Research Paper, No. 68, 1960.
45. Trimpi, Robert L., Grant, Frederick C., and Cohen, Nathaniel B.: Aerodynamics and Heating Problems of Advanced Reentry Vehicles. Vol. 2, Proc. NASA-University Conference on Science and Technology of Space Exploration. NASA SP-11, no. 53, 1962, pp. 235-248.
46. Allen, H. Julian: Gas Dynamics Problems of Space Vehicles. Vol. 2, Proc. NASA-University Conference on the Science and Technology of Space Exploration. NASA SP-11, no. 54, 1962, pp. 251-267.
47. Howe, John T., and Shaeffer, Yvonne S.: Mass Addition in the Stagnation Region for Velocity up to 50,000 Feet/Second. NASA TR R-207, 1964.
48. Hearne, L. F., Chin, Jin H., and Lefferdo, J. M.: Reentry Heating and Thermal Protection of a Mars-Mission Earth-Reentry Module. Presented at the AIAA Entry Technology Conference, Oct. 12-14, 1964, Williamsburg, Va. (AIAA Publication CP-9), pp. 118-135.

49. Allen, H. Julian: The Aerodynamic Heating of Atmosphere Entry Vehicles - A Review. Presented at the Symposium on Fundamental Phenomena in Hypersonic Flow, June 25-26, 1964, Buffalo, N.Y.
50. Tauber, Michael E., and Seiff, Alvin: Optimization Analysis of Conical Bodies Making Lifting Hyperbolic Entries into the Atmospheres of Earth and Mars. Presented at the AIAA Entry Technology Conference, Oct. 12-14, 1964, Williamsburg, Va., (AIAA Publication CP-9, pp. 13-21).
51. Canning, Thomas N., and Page, William A.: Measurements of Radiation from the Flow Fields of Bodies Flying at Speeds up to 13.4 Kilometers per Second. Presented to the Fluid Mechanics Panel of AGARD, April 3-6, 1962, Brussels, Belgium.
52. Trimpi, Robert L., and Callis, Linwood B.: A Perfect-Gas Analysis of the Expansion Tunnel, a Modification to the Expansion Tube. NASA TR R-223, 1965.
53. Trimpi, Robert L.: A Preliminary Theoretical Study of the Expansion Tube, a New Device for Producing High-Enthalpy Short-Duration Hypersonic Gas Flows. NASA TR R-133, 1962.
54. Vorreiter, John W., and Shepard, Charles E.: Performance Characteristics of the Constricted-Arc Supersonic Jet. Proceedings of the 1965 Heat Transfer and Fluid Mechanics Institute, Stanford University Press, 1965, pp. 42-49.

PROBES

MANNED MARS MISSIONS

PLANET	VELOCITY, km/sec
VENUS	11 OR GREATER
MARS	6 OR GREATER
JUPITER	APPROX 60

ENTRY MODE	VELOCITY, km/sec
DIRECT MARS ENTRY	6 TO 11
MARS ENTRY FROM ORBIT	3.6 TO 5.2
EARTH ENTRY	12 TO 16

Figure 1.- Characteristic entry velocities for future missions.

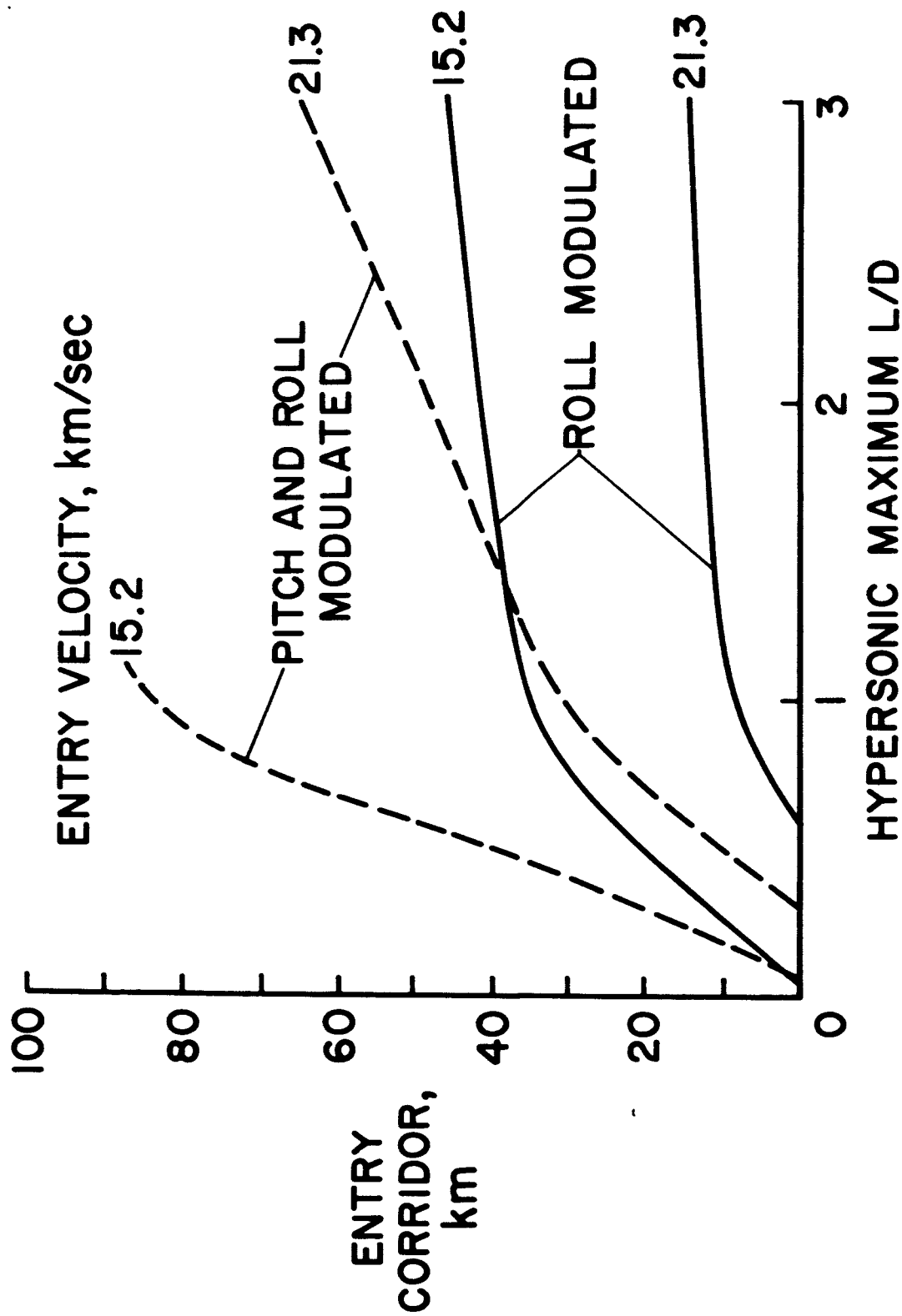
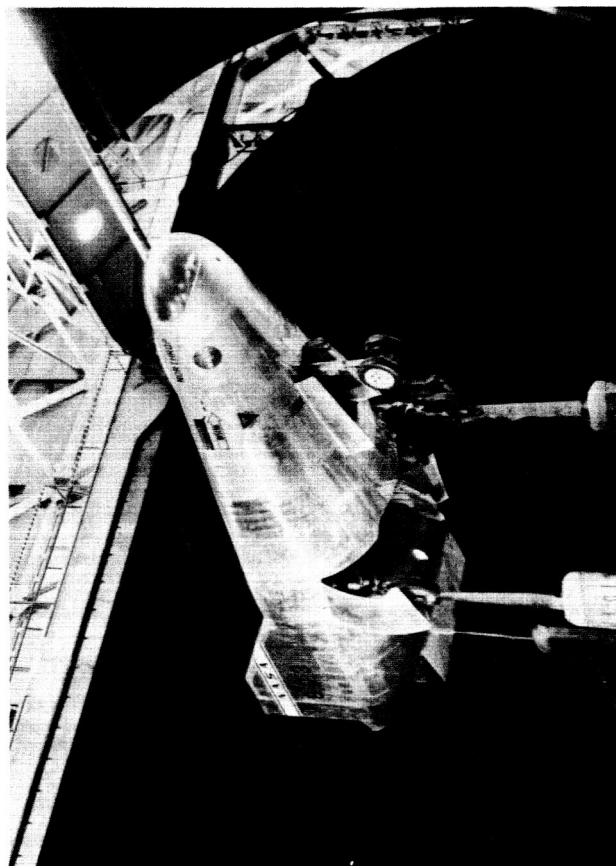


Figure 2.- Earth entry corridor as a function of hypersonic maximum lift-drag ratio.



A-35069

Figure 3.- Low-speed lifting reentry research vehicle.

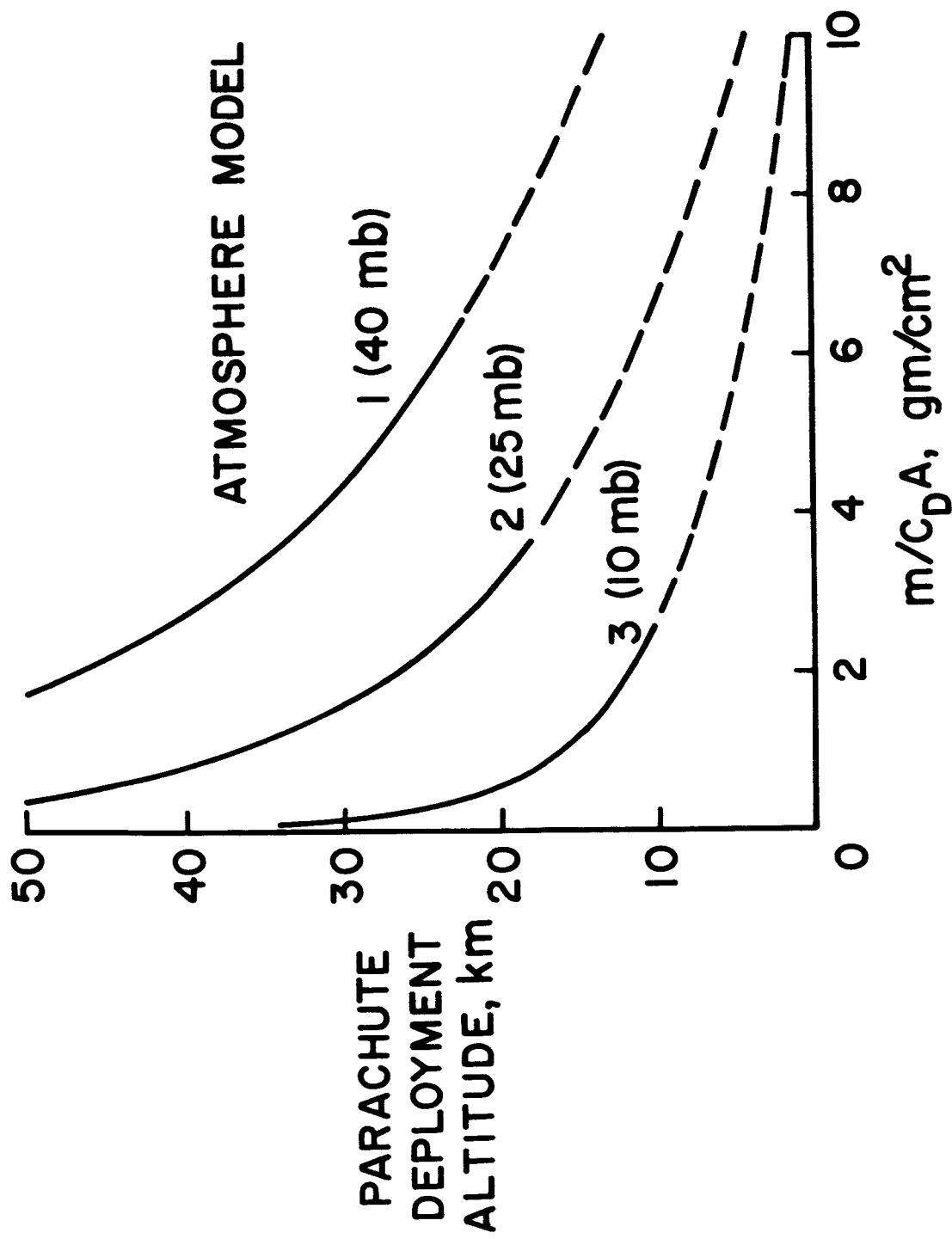


Figure 4.- Parachute deployment altitude as a function of ballistic parameter for three model atmospheres of Mars, $V/V_E = 0.05$.

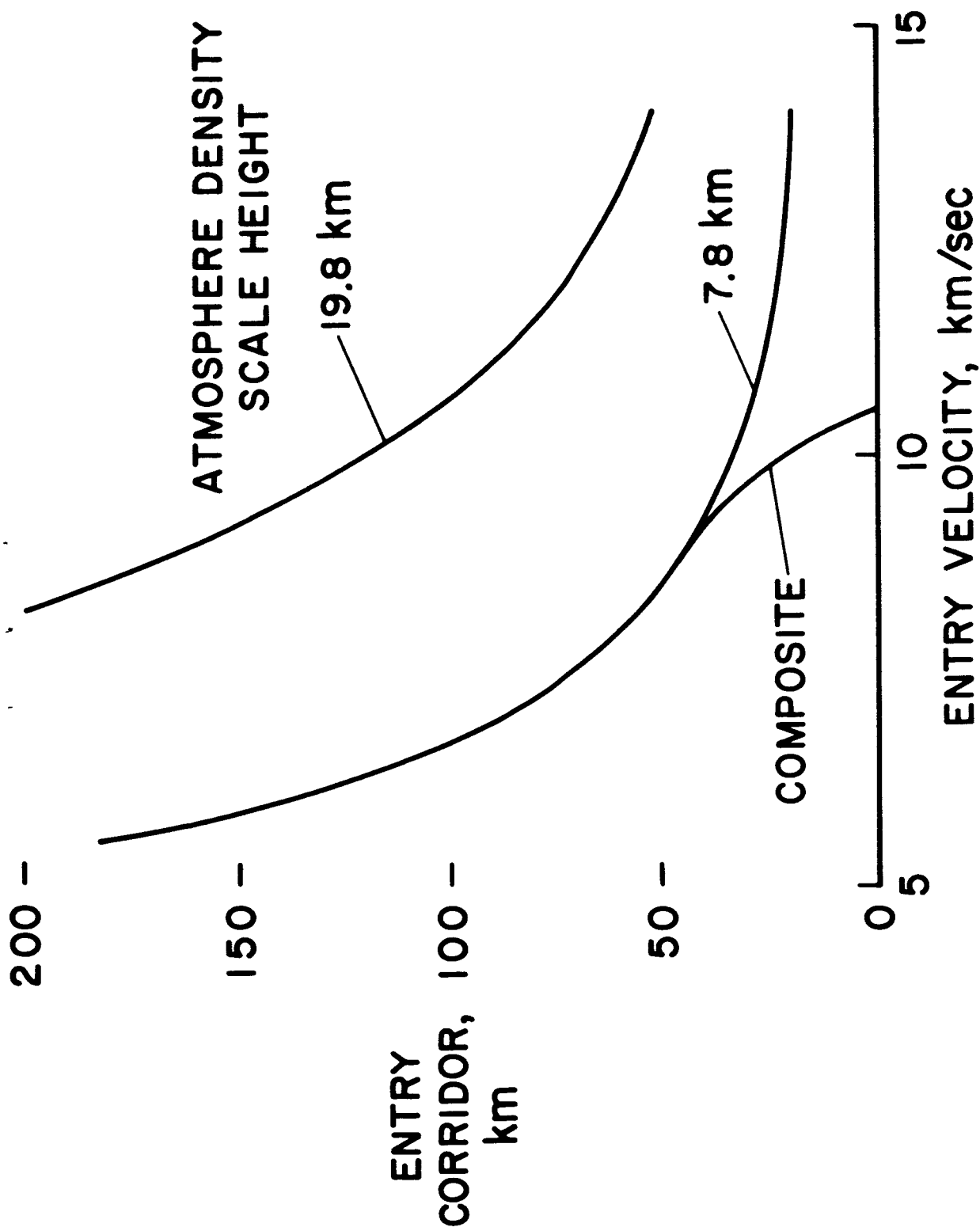


Figure 5.- Mars entry corridor as a function of entry velocity for various scale heights, $L/D \approx 1/2$.

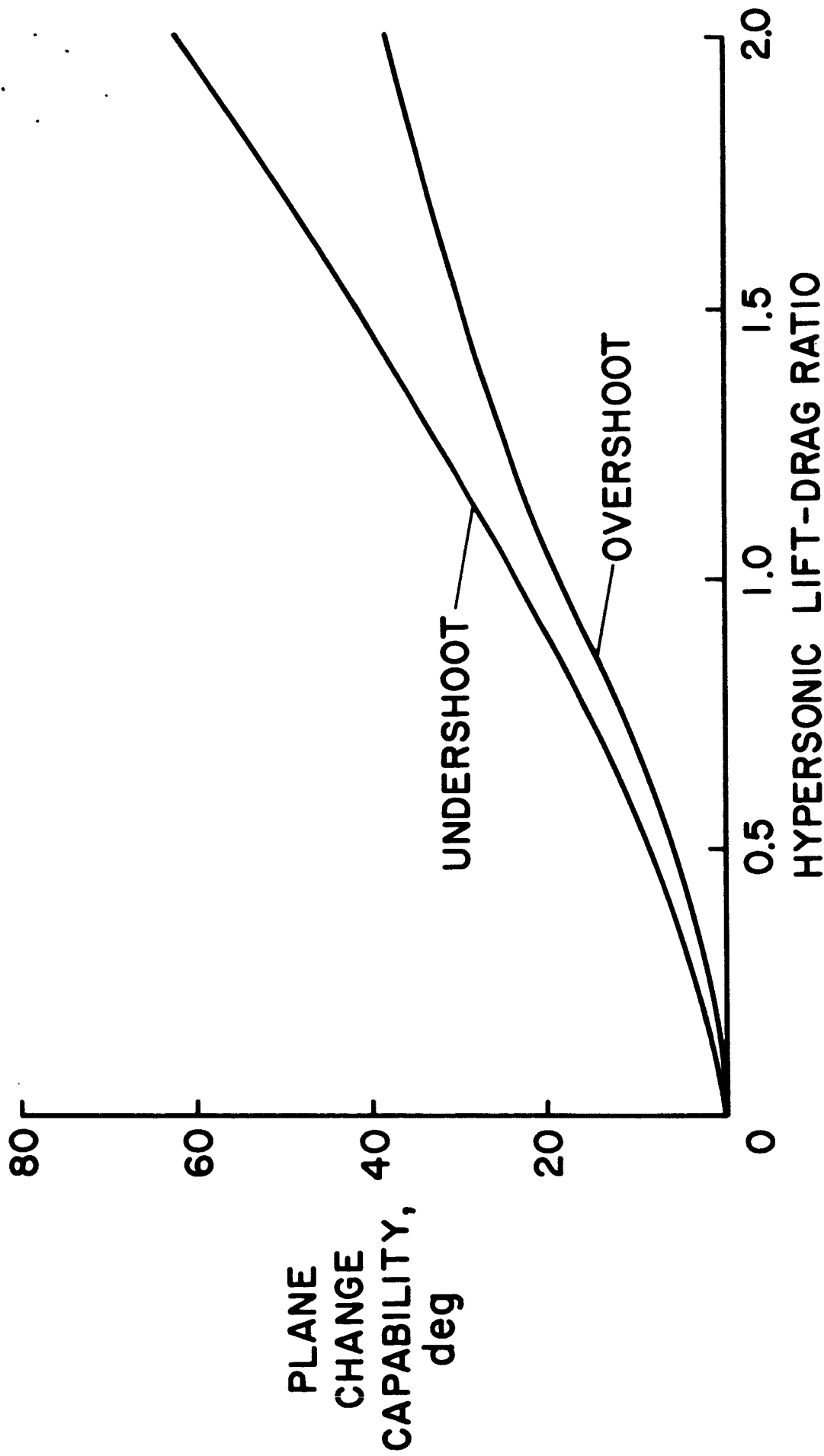


Figure 6.- Aerodynamic plane change capability for Mars entry and skip out to orbit as a function of hypersonic lift-drag ratio, $V_E = 8.4$ km/sec.

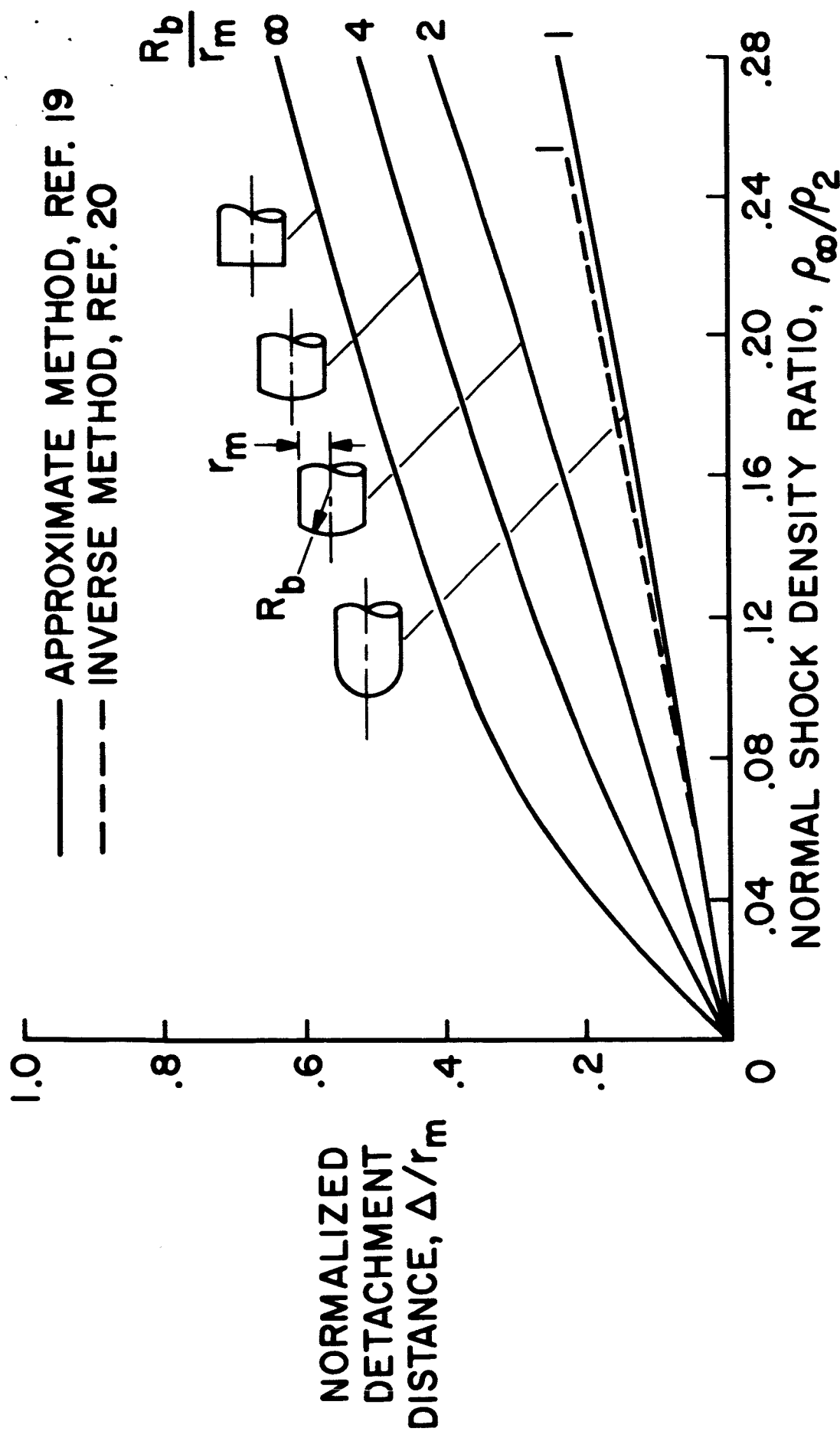
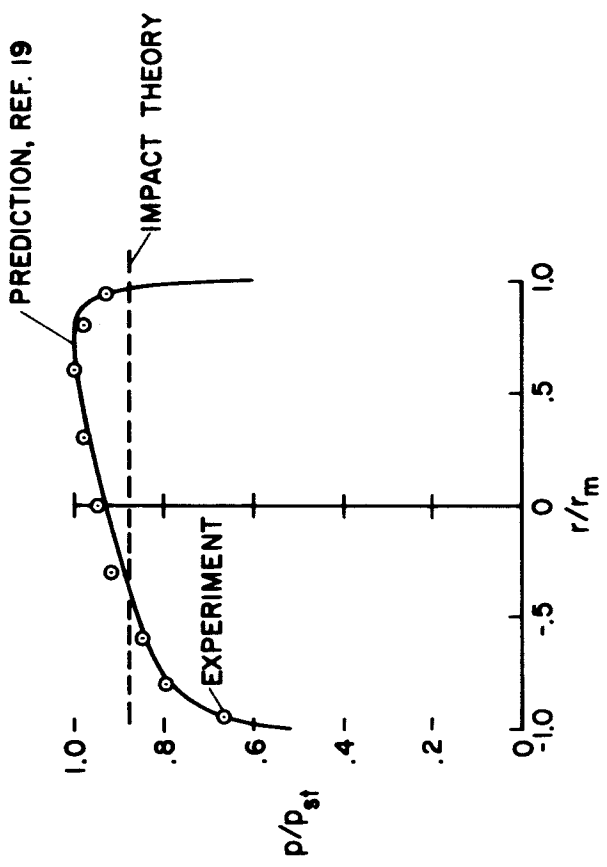
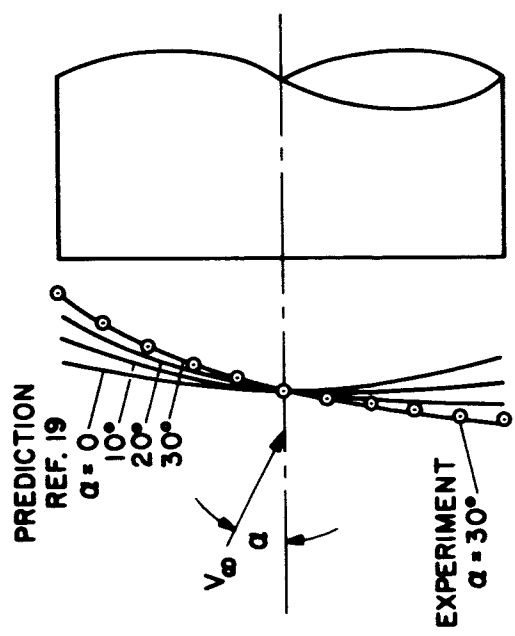


Figure 7.- Stagnation-point shock detachment distance as a function of normal shock density ratio for a family of spherically blunted cylinders.



(b) Pressure distribution, $\alpha = 20^\circ$.



(a) Shock shape.

Figure 8.- Shock shape and pressure distribution for flat-faced cylinder at angle of attack.

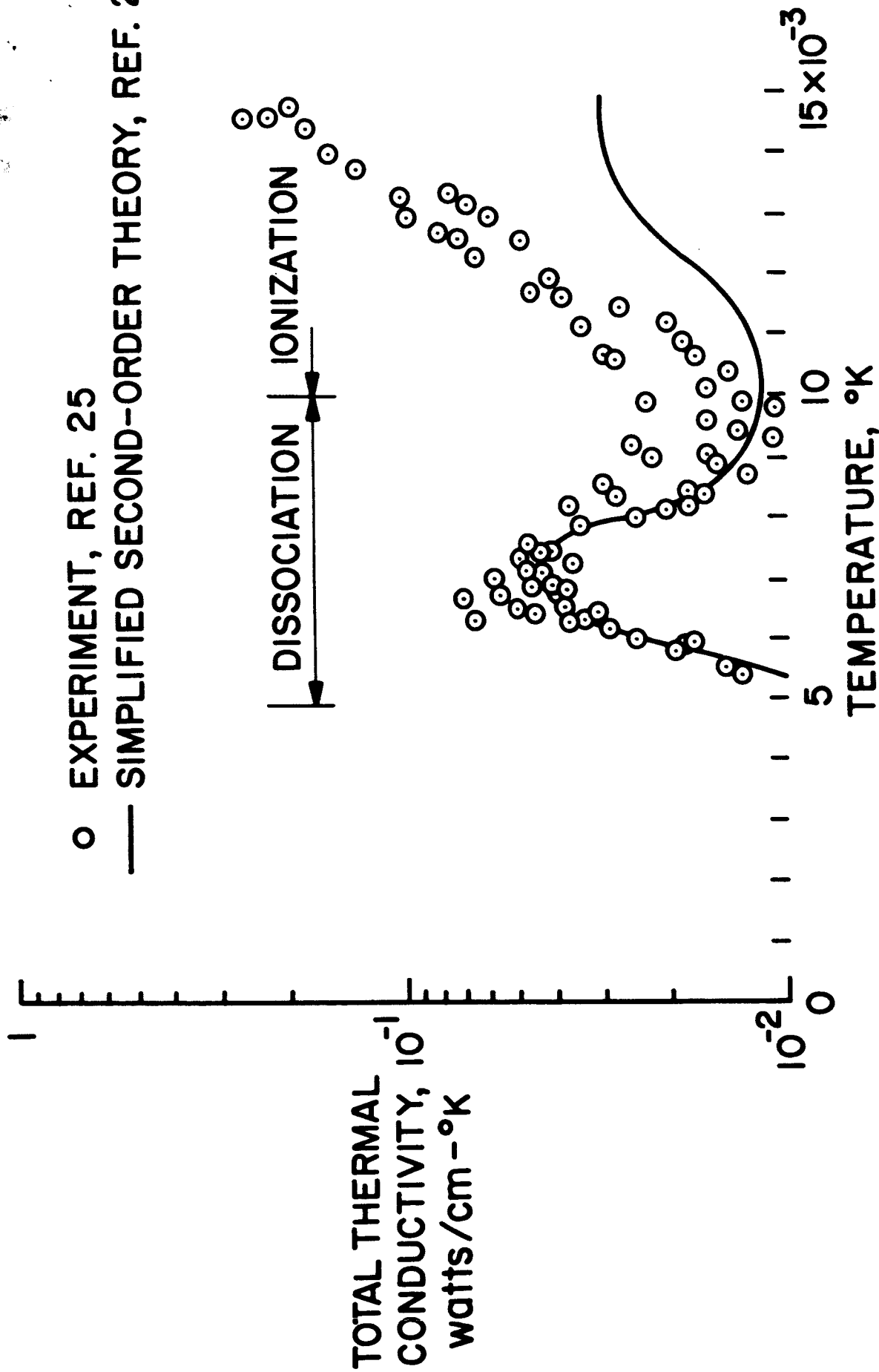


Figure 9.- Total thermal conductivity of nitrogen as a function of temperature at 1 atmosphere pressure - experiment and simplified theory.

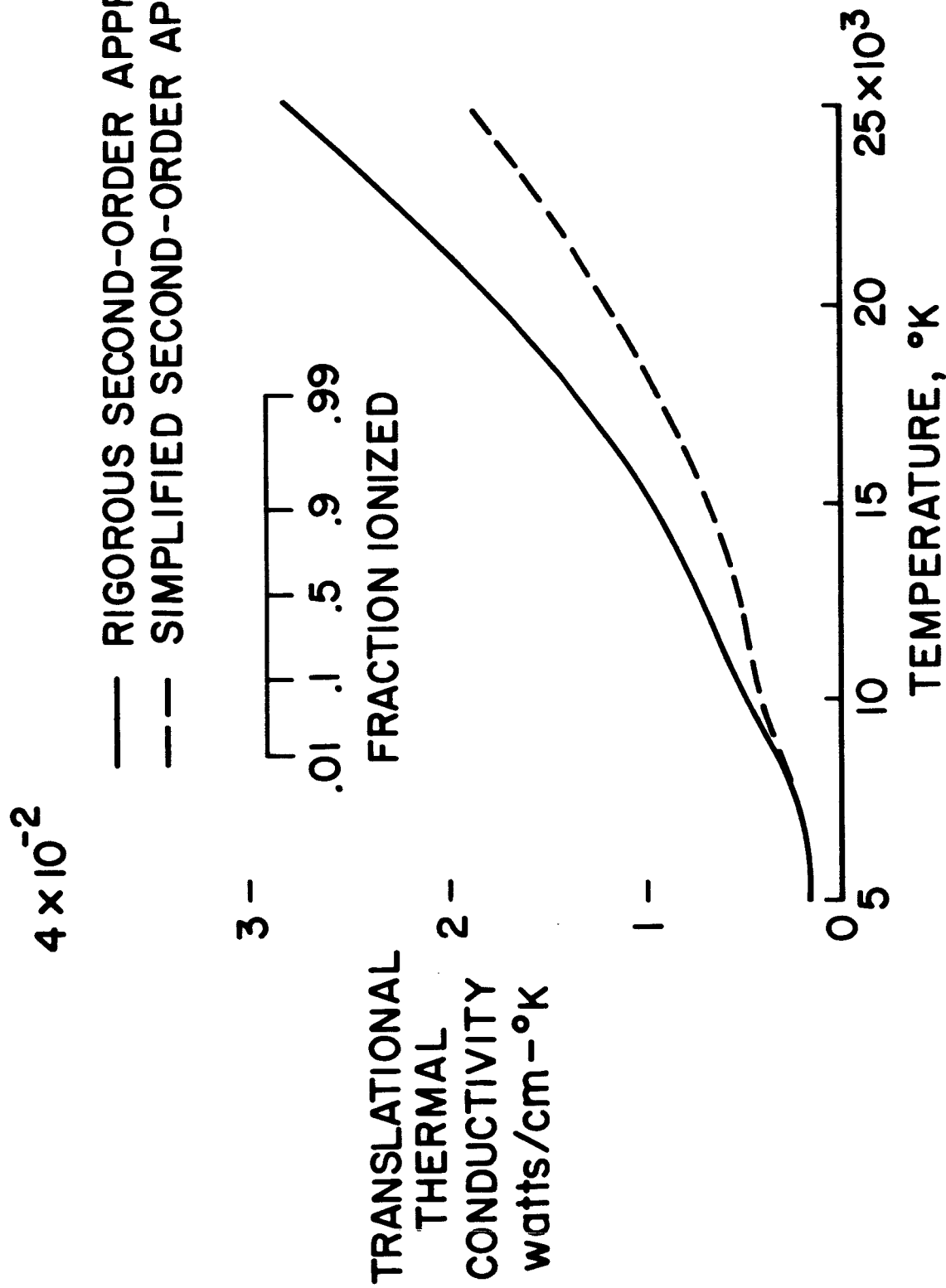


Figure 10.- Comparison of simplified and rigorous second-order approximations for translational thermal conductivity of argon, 10^{-1} atmosphere.

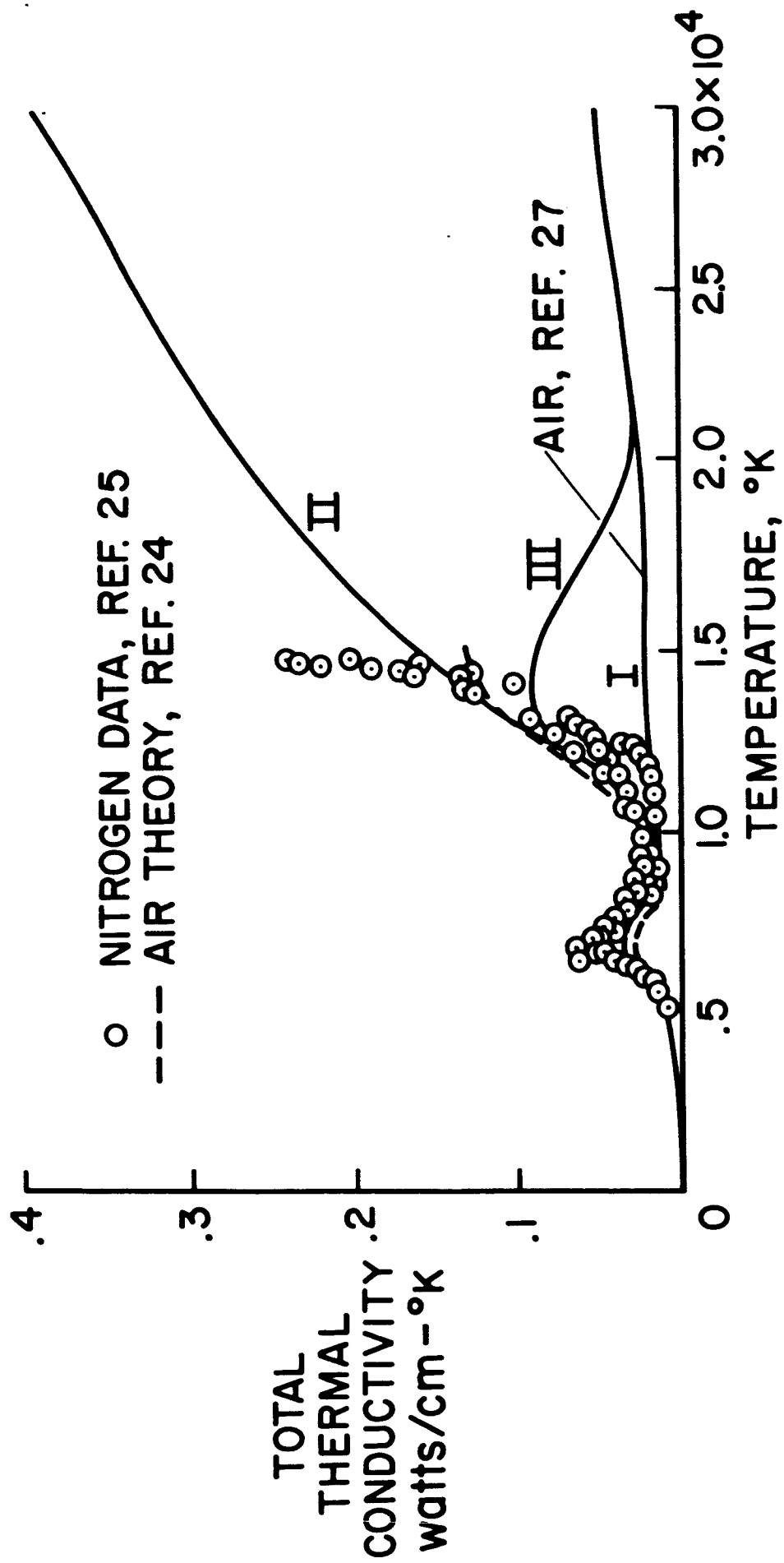


Figure 11.- Total thermal conductivity of air as a function of temperature; arbitrary extrapolations, 1 atmosphere.

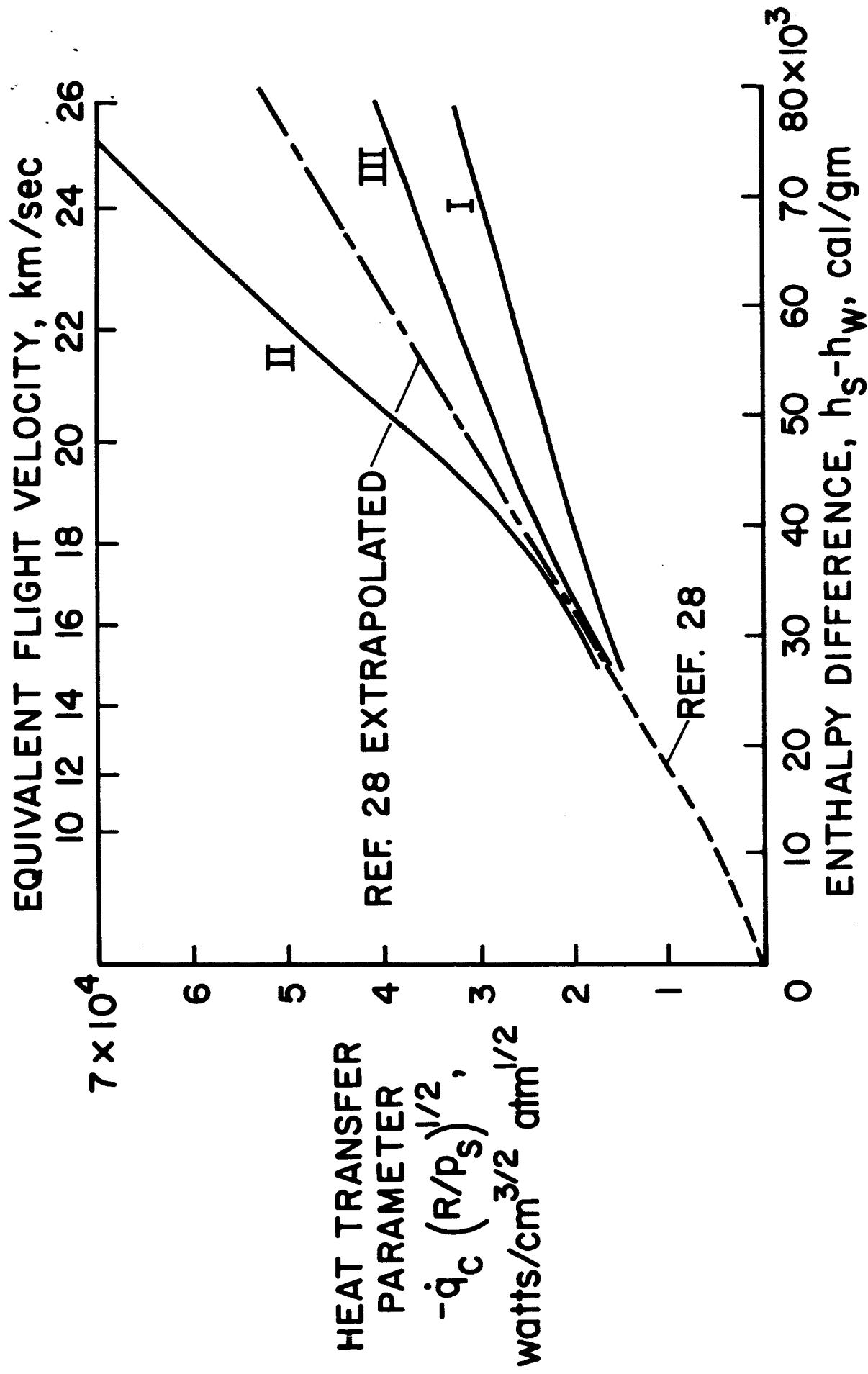


Figure 12.- Stagnation-point convective heat-transfer parameter for three different assumed total thermal conductivities of ionized air.

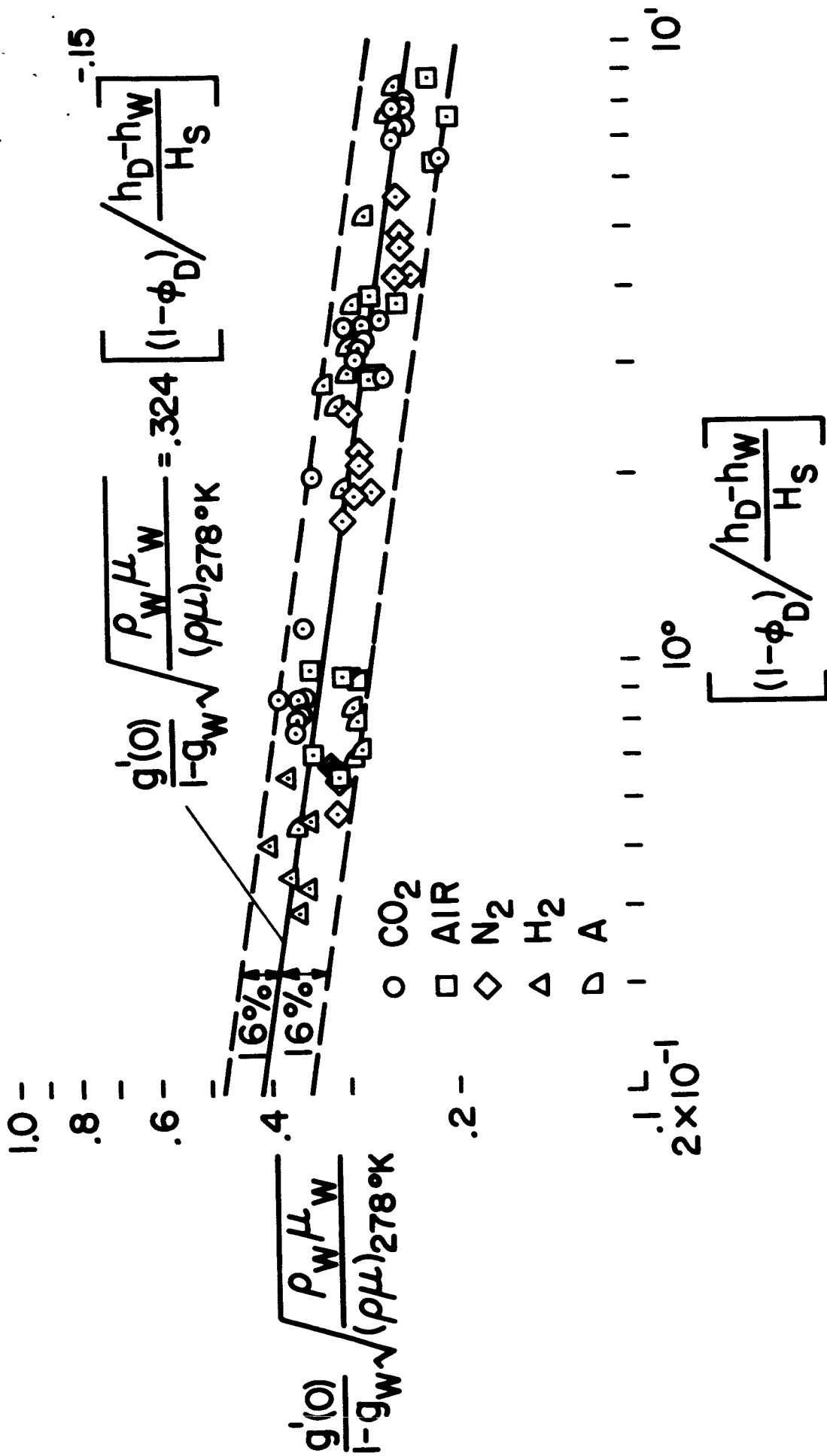


Figure 13.- Correlation of stagnation heat transfer for a number of gases.

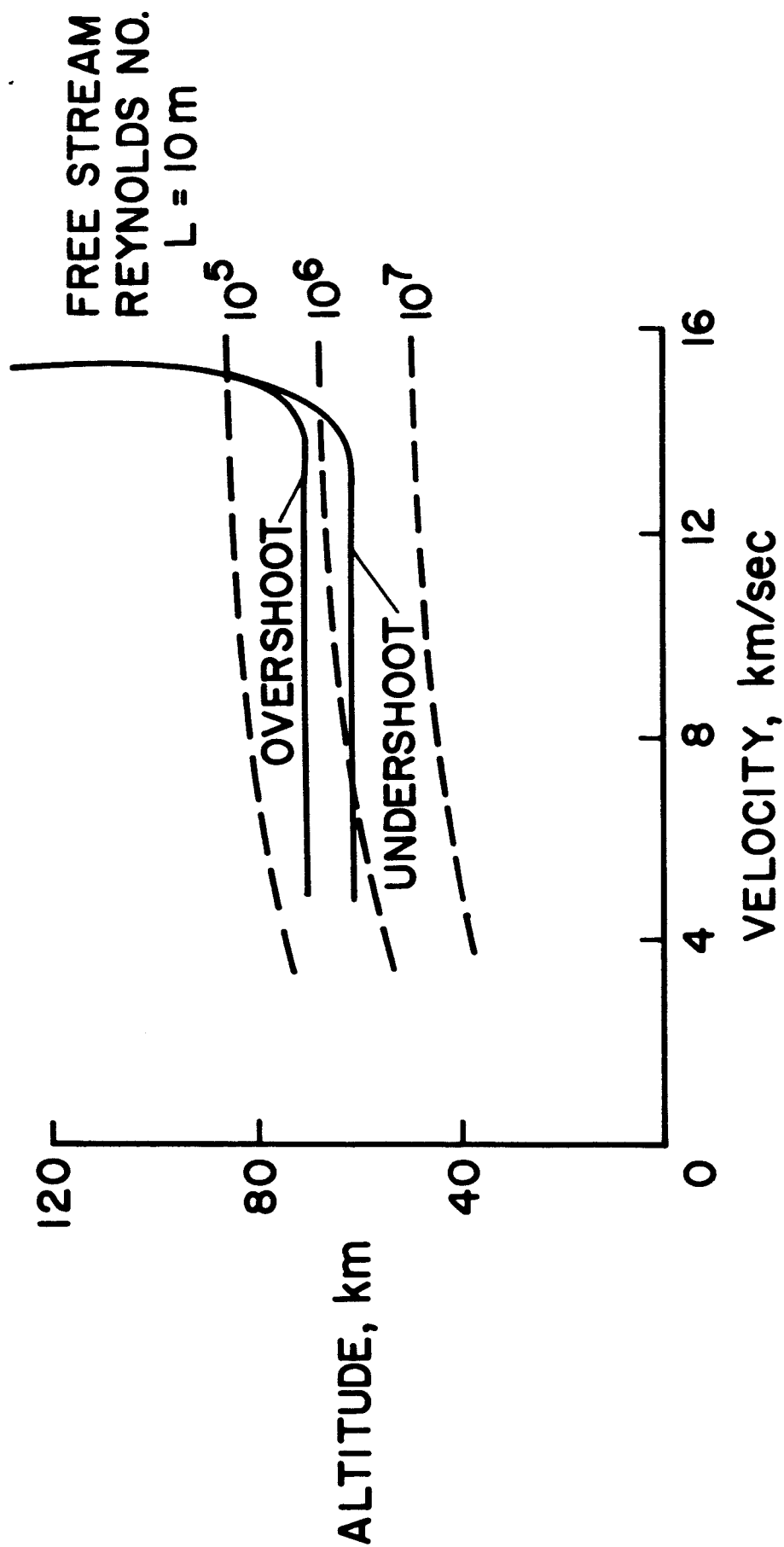


Figure 14.- Reynolds number flight regime for typical hyperbolic earth entry; $V_E = 15.2 \text{ km/sec}$, $L/D = 1$.

DATA

○ REF. 34, 9% CO₂-91% N₂, $p_{\infty}/p_0 = .018-.12$

□ REF. 36, 7-1/2% CO₂-92-1/2% N₂, $p_{\infty}/p_0 = .08$

◇ REF. 37, 9% CO₂-91% N₂, $p_{\infty}/p_0 = .001-.04$

△ REF. 38, 9% CO₂-90% N₂-1% A, $p_{\infty}/p_0 = .002-.02$

EMISSION
PARAMETER

$E/(p/p_0)^{1.55}$

watts/cm³

PREDICTIONS

— REF. 34, 9% CO₂-91% N₂, $p_{\infty}/p_0 = .018-.12$

--- (MOLECULAR RADIATORS ONLY)

--- REF. 37, 9% CO₂-91% N₂, $p_{\infty}/p_0 = .01$

(INCLUDES CONTINUUM)

▨ REF. 35, AIR, $p_{\infty}/p_0 = .013-.08$

VELOCITY, km/sec

10⁸ —

10⁶ —

10⁴ —

10² —

10⁰ L
5

6

7

8

9

10

11

12

13

Figure 15.- Equilibrium radiation from a CO₂-N₂ mixture.

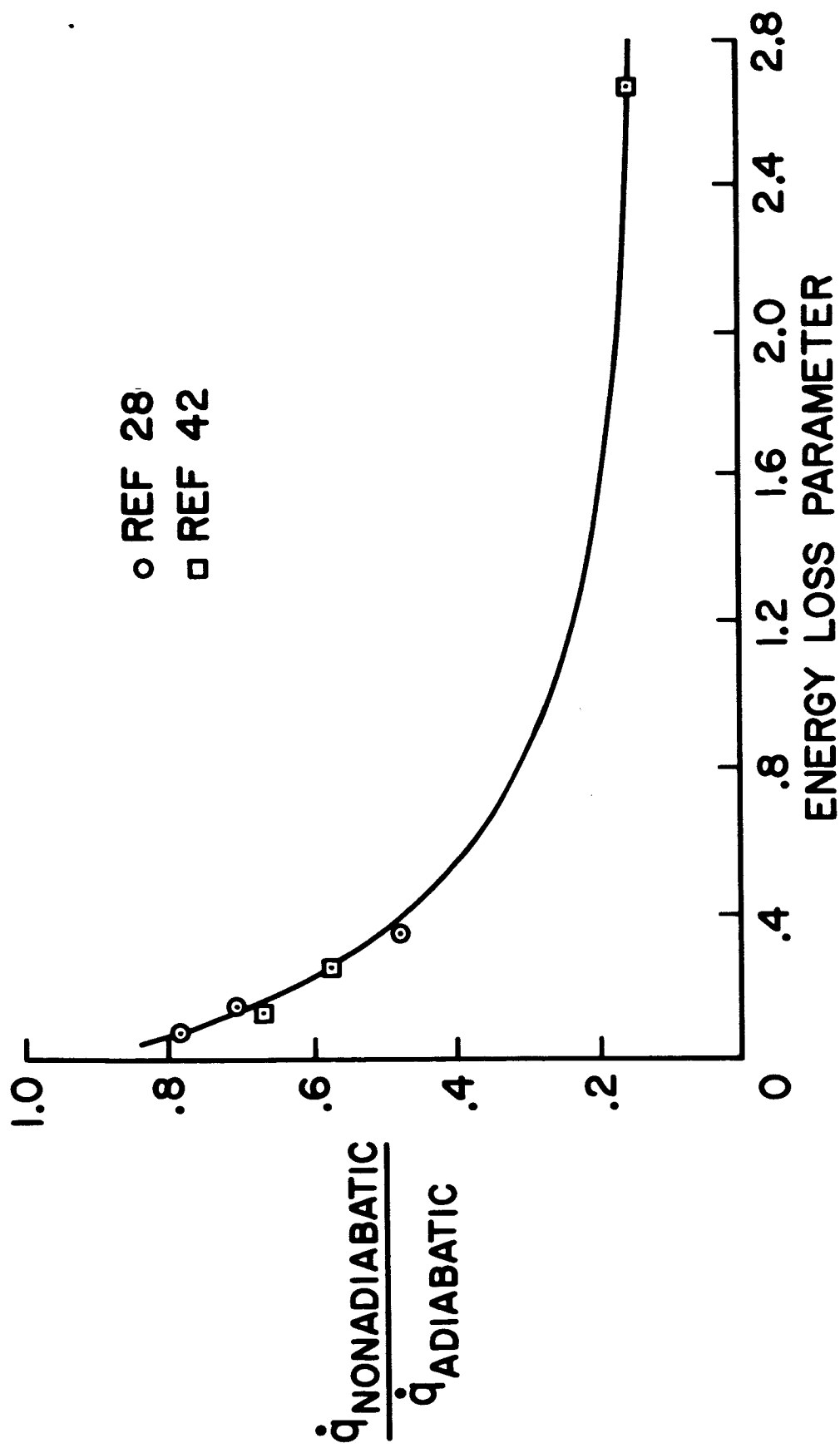


Figure 16. - Reduction in stagnation radiative heat-transfer rate as a function of energy loss parameter.

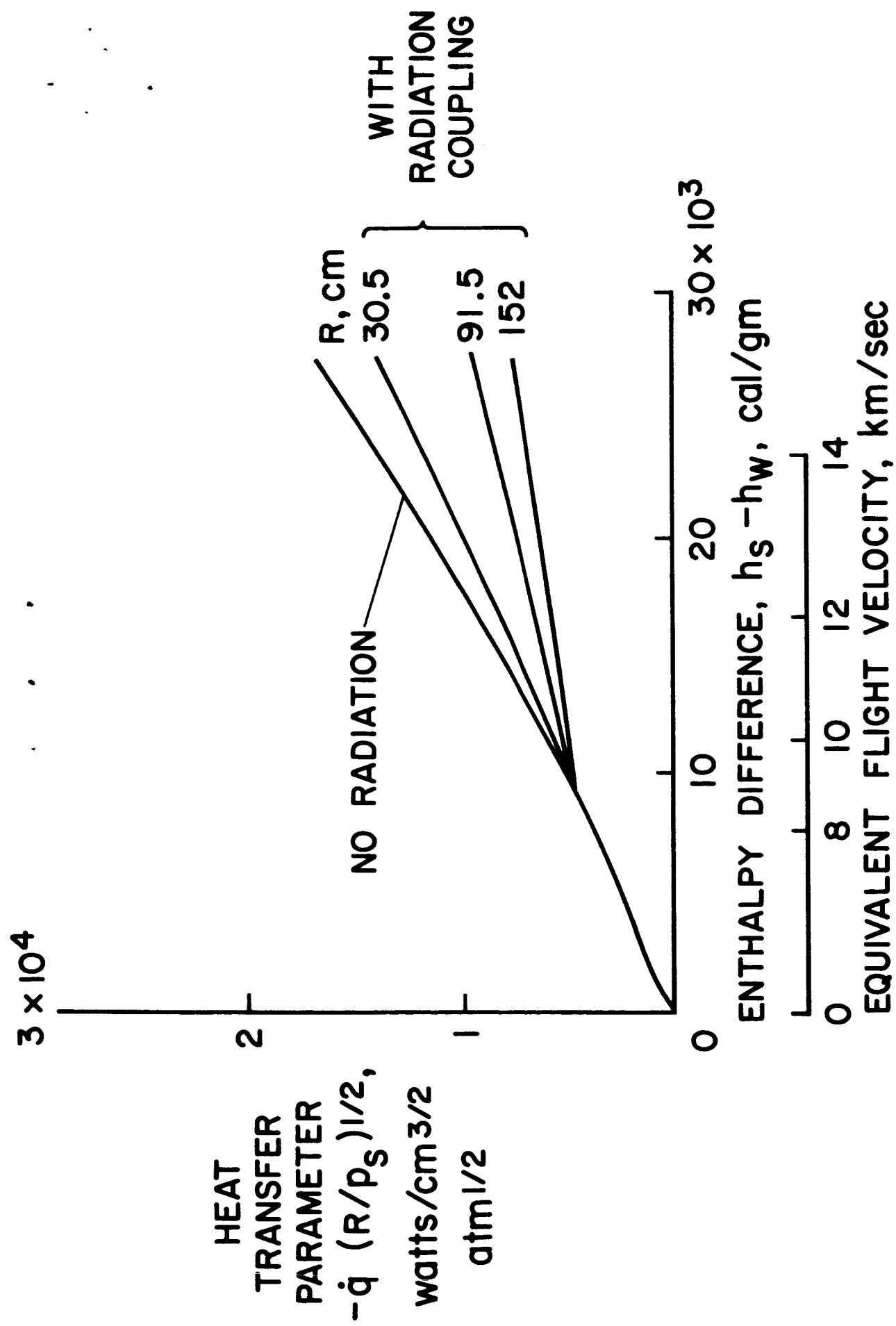


Figure 17.- Effect of radiation energy loss on convective stagnation-point heat-transfer rate, 1 atmosphere pressure.

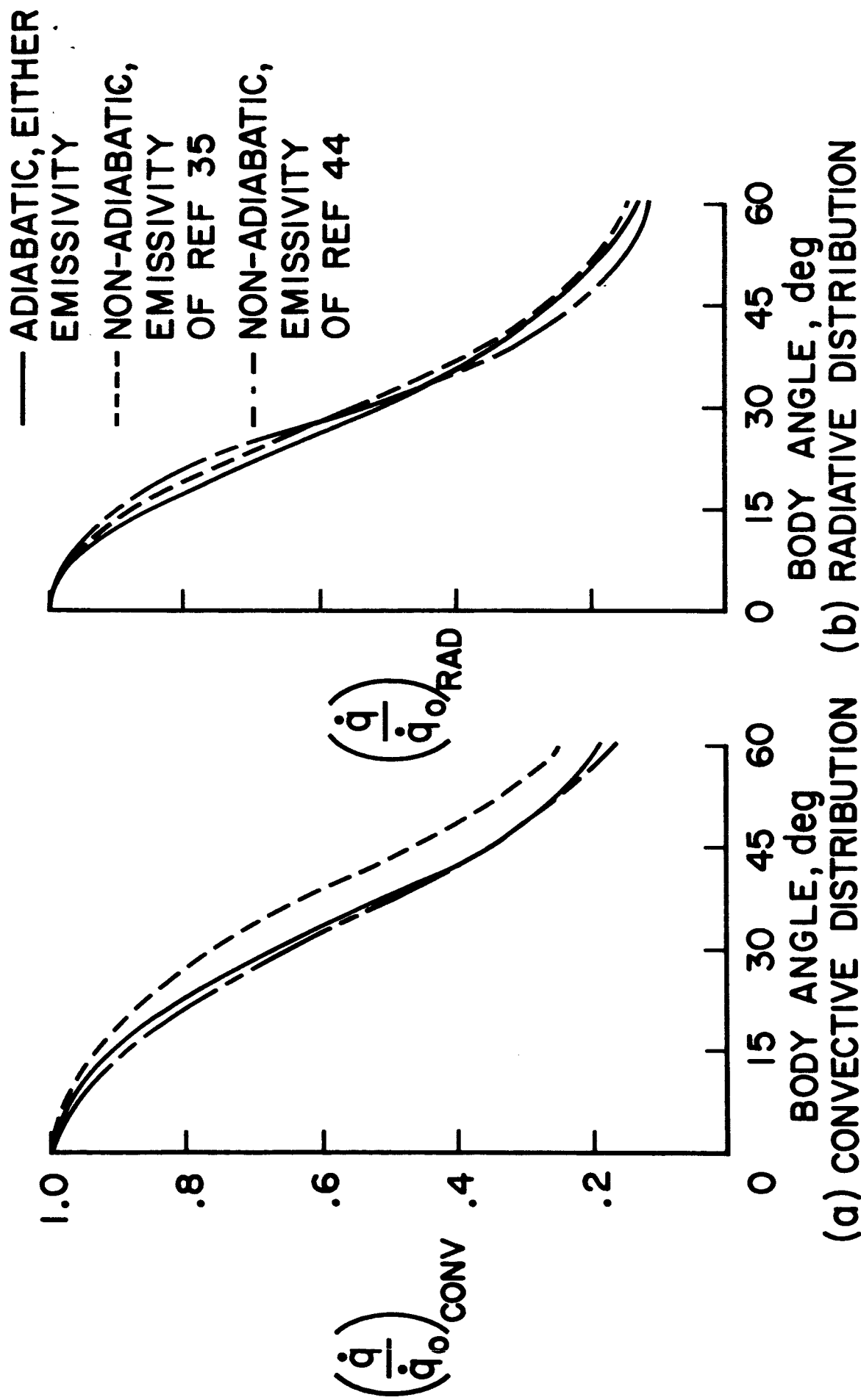
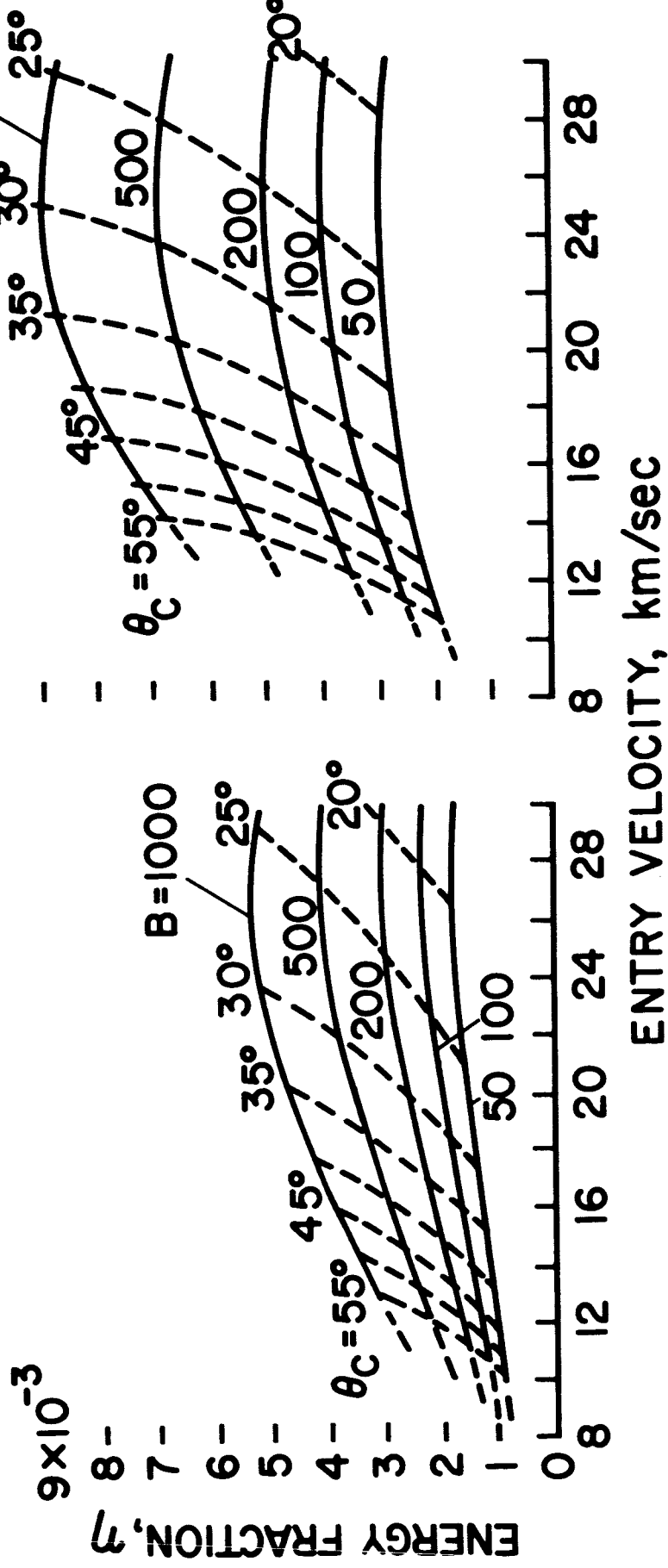


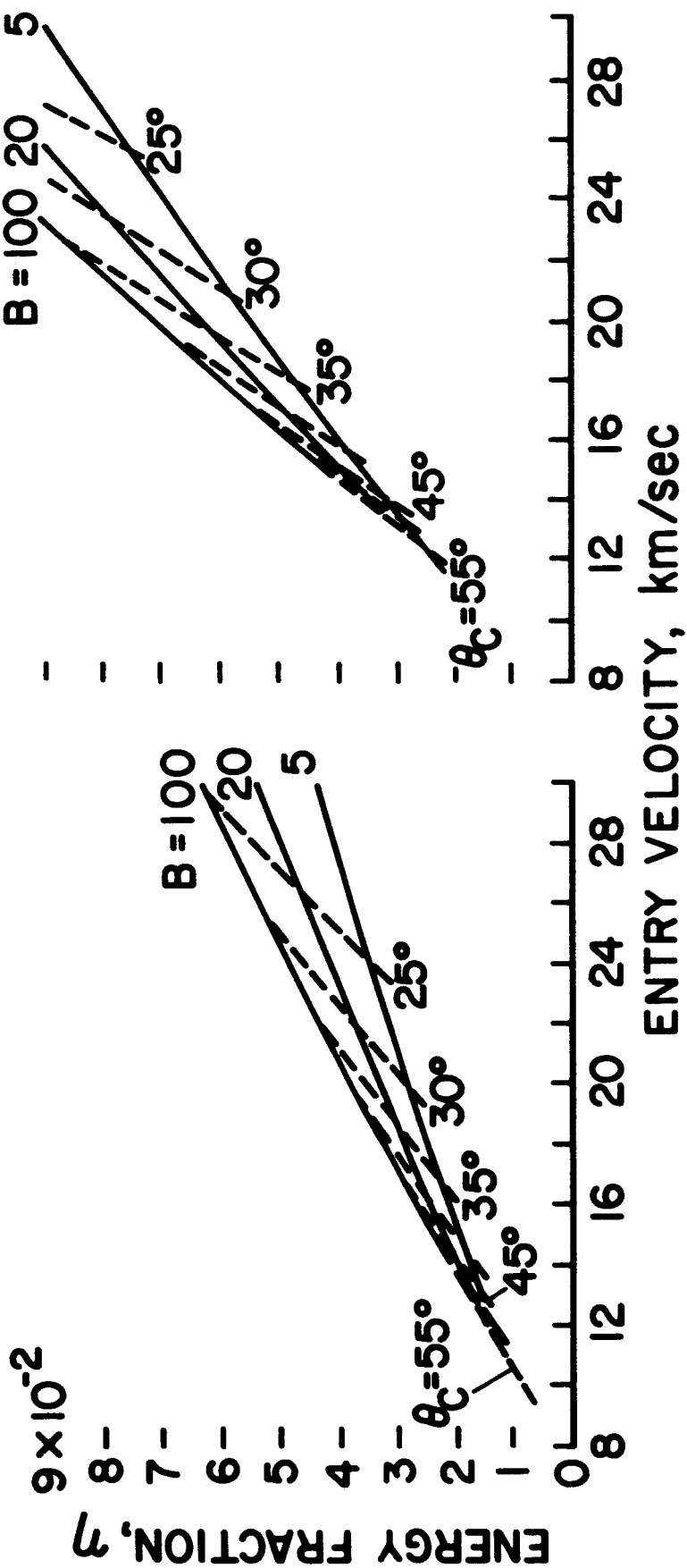
Figure 12.- Effect of radiative cooling on convective and radiative heat-transfer distributions for a hemisphere; $V = 15.2$ km/sec, altitude = 50 km, radius = 1.52 m.



(a) Teflon ablator.

(b) Vaporizing quartz ablator.

Figure 19.- Minimum absorbed energy fractions for optimum cones with all laminar flow.



(a) Teflon ablator.

(b) Vaporizing quartz ablator.

Figure 20.- Minimum absorbed energy fractions for optimum cones with all turbulent flow.

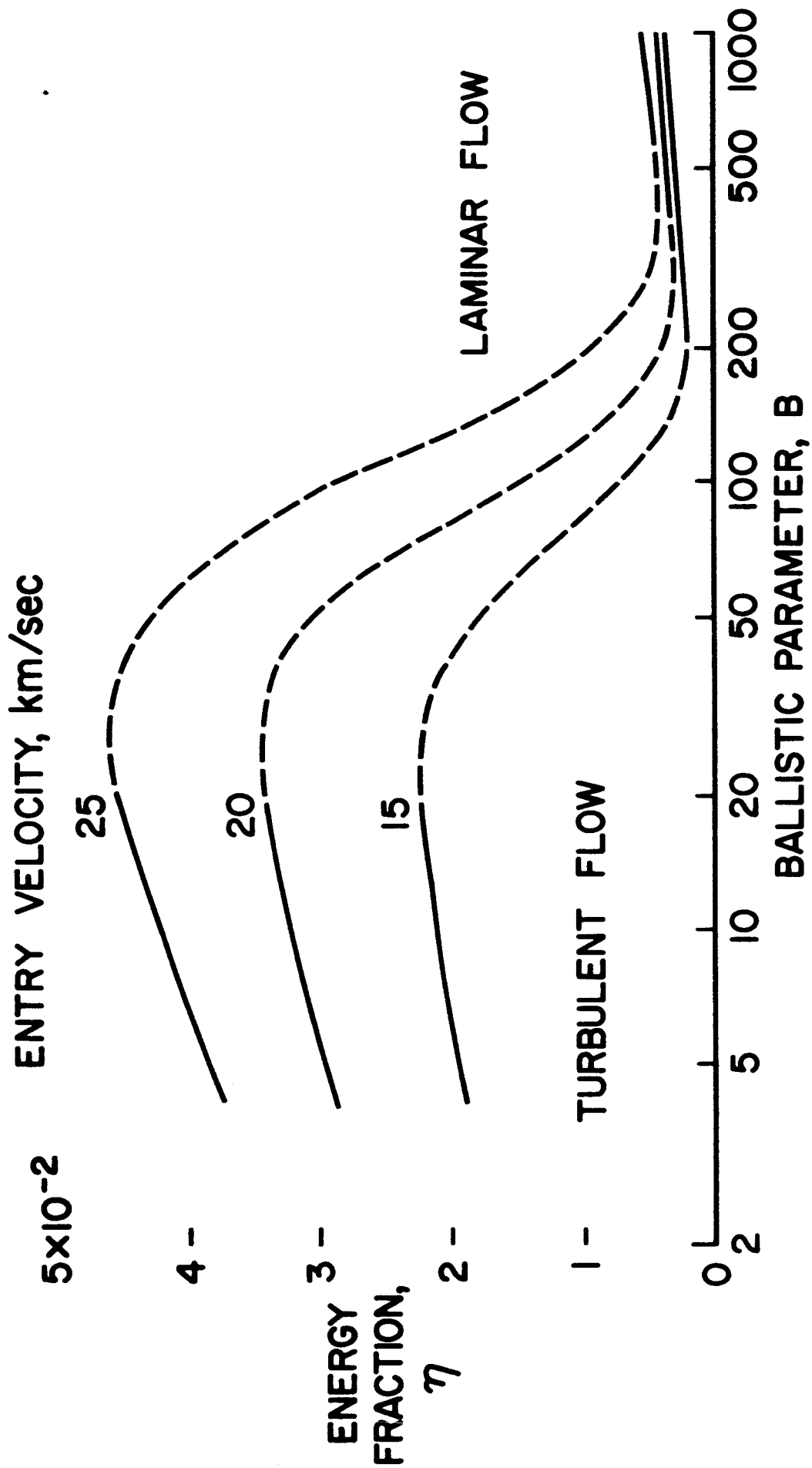


Figure 21.- Variation of minimum absorbed energy fraction with ballistic parameter for several entry velocities, teflon ablator.

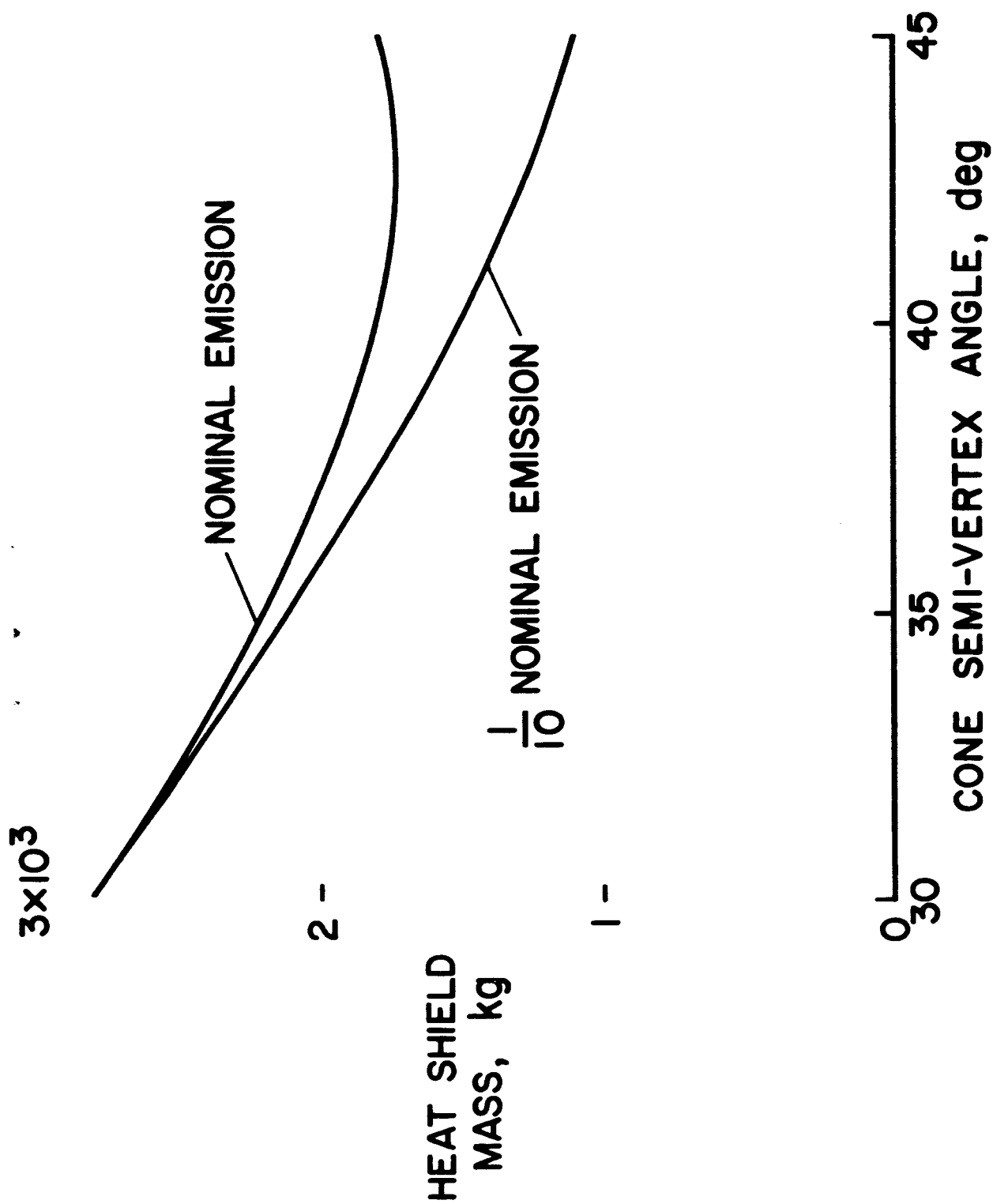


Figure 22.- Heat-shield mass as a function of cone semivertex angle for a lifting entry vehicle; $L/D = 0.6$, $V_E = 19.8$ km/sec. Effect of level of emission.

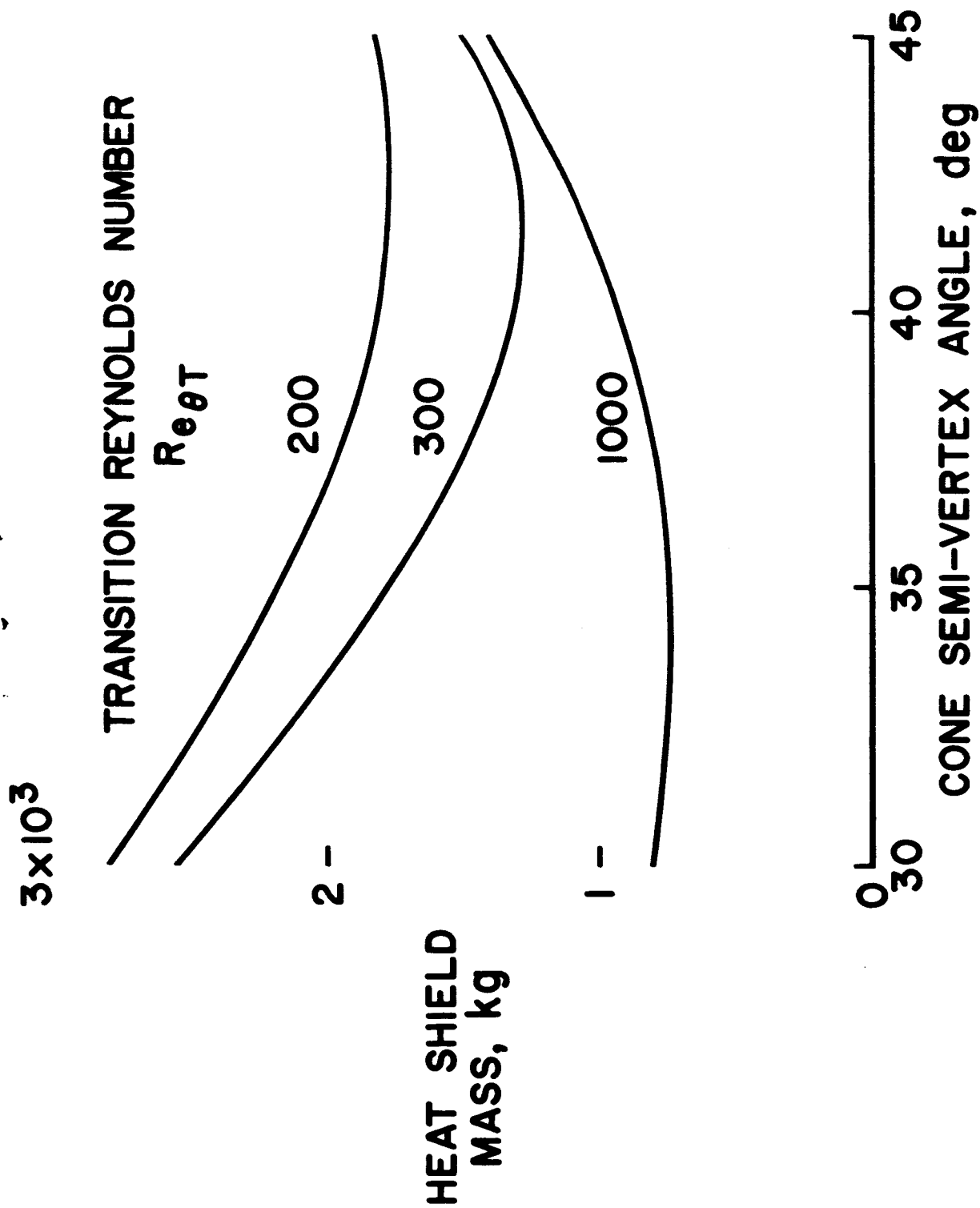


Figure 23.- Heat-shield mass as a function of cone semivertex angle for a lifting entry vehicle; $L/D = 0.6$, $V_E = 19.8$ km/sec. Effect of transition Reynolds number.

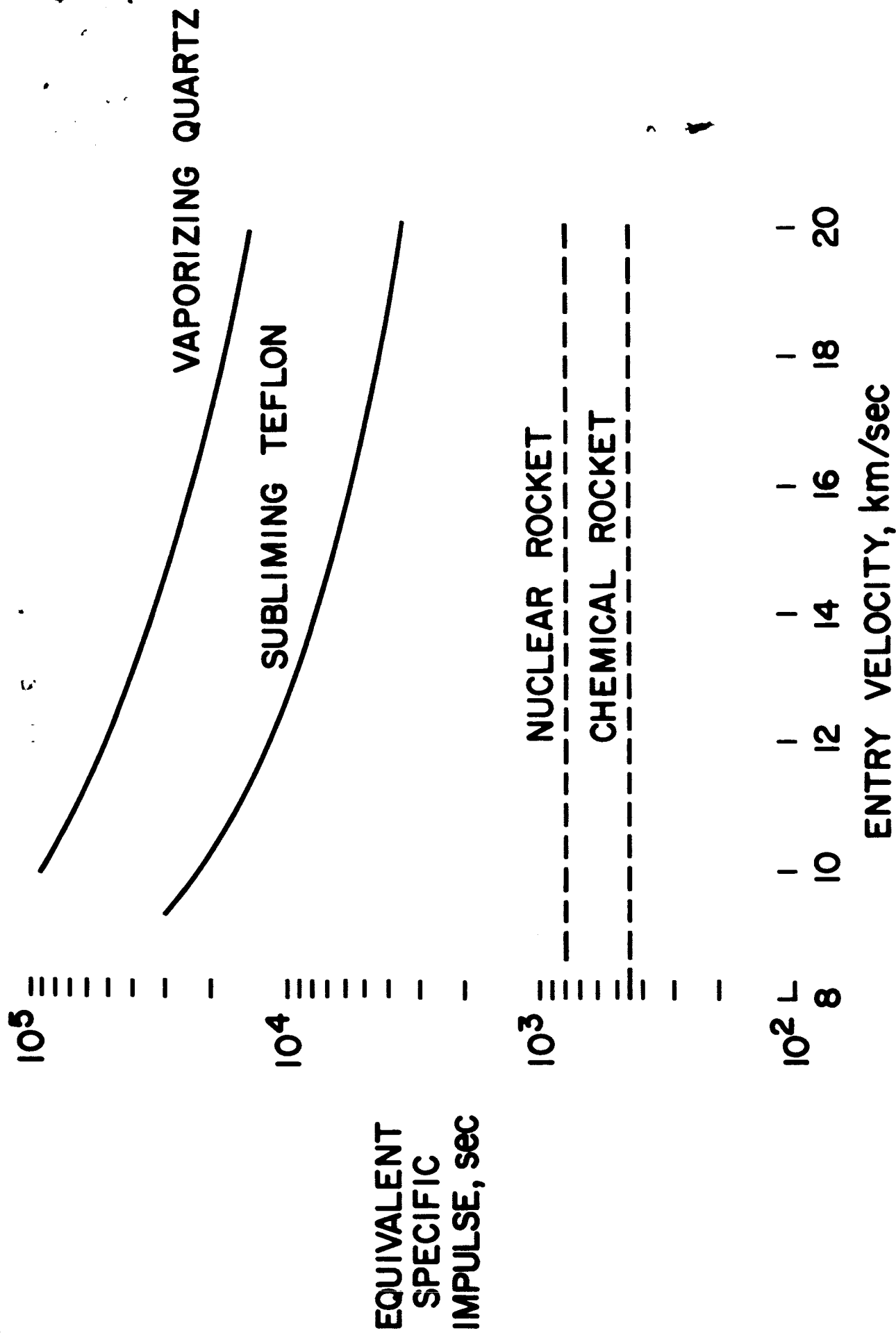


Figure 24.- Equivalent specific impulse of aerodynamically braked vehicle, laminar flow.